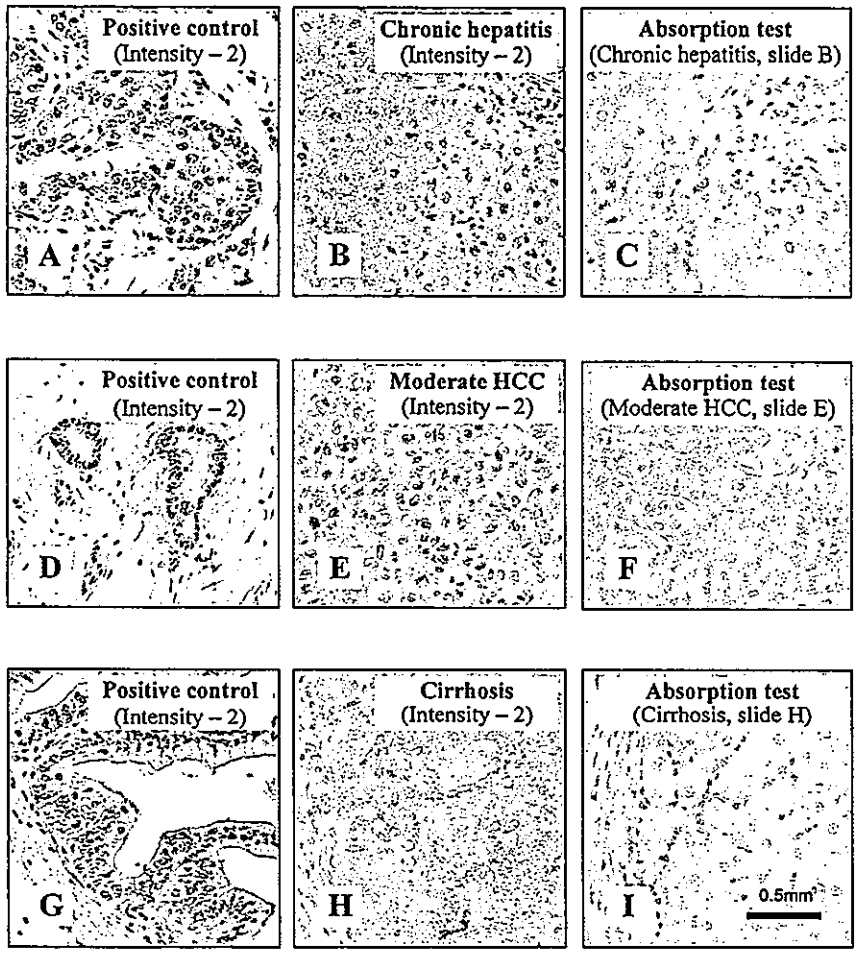

Figure 1. Positive control and antibody specificity test for Id1 (A-C), Id2 (D-F) and Id3 (G-I) proteins. Tissue processing, immunostaining and intensity evaluation were performed as described in Materials and methods. For positive controls, sections of breast cancer expressing Id1 protein (A) (14), and sections of pancreatic cancer expressing Id2 (D) or Id3 protein (G) (12) were included in the respective staining procedures. The positive controls displayed moderate (intensity-2) cytoplasmic staining. Pre-absorbed antibodies with an excess amount of Id1-, Id2- or Id3-specific blocking peptides, completely abolished immunostaining on the sections of the respective primary antibody (C is the absorption test of B for Id1 antibody; F, the absorption test of E for Id2 antibody; and I, the absorption test of H for Id3 antibody). In the negative controls, when the primary antibodies were substituted by TBS, no staining was observed (data not shown). (Original magnification x400).

resected specimens of HCC (19). The present study extends their findings. We examined Id1, Id2 and Id3 expression and those correlations with clinicopathological factors in HCCs with surrounding HCV or HBV-related chronic hepatitis and liver cirrhosis.

Materials and methods

Patients and tissue samples. Formalin-fixed, paraffin-embedded liver tissue specimens were prepared from 54 patients with HCC (44 males and 10 females; ranging in age from 36 to 76 years; mean, 61.0 years), who underwent hepatectomy at the Department of Surgery and Clinical Oncology, Osaka University between 1994 and 2000. Most of the patients (87%) had either HCV infection (29 patients) or HBV infection (16 patients) and 2 patients had concomitant infection with HCV and HBV. Adjacent non-tumor liver tissues were either chronic hepatitis (n=30) or liver cirrhosis (n=24). Of the carcinoma tissues, 45 of 54 HCCs were evaluated, because 9 samples of HCC were found to be completely necrotic, due to preoperative transarterial embolization therapy. Based on histopathological examination 8 cases were diagnosed as well-differentiated, 18 as moderately-differentiated, 15 cases as poorly-differentiated and 4 cases as undifferentiated HCC. The study protocol was approved by the Human Ethics Review Committee of Osaka University, Graduate School of Medicine and a signed consent form was obtained from each subject.

Antibodies. Specific rabbit anti-human Id1 (sc-488), Id2 (sc-489) and Id3 (sc-490) (Santa Cruz Biotechnology, Santa Cruz, CA) polyclonal antibodies were used for immunohistochemistry and Western blotting. These affinity-purified rabbit polyclonal antibodies specifically react with the carboxy terminus of the respective Id1, Id2 and Id3 protein. Blocking peptides for Id1 (sc-488P), Id2 (sc-489P) and Id3 (sc-490P) (Santa Cruz Biotechnology) were used for absorption tests.

Western blot analysis. Approximately 50 mg of liver tissue was homogenized in 0.5 ml ice-cold RIPA buffer [25 mM Tris (pH 7.5), 50 mM NaCl, 0.5% sodium deoxycholate, 2% Nonidet P-40, 0.2% sodium dodecyl sulfate, 1 mM phenylmethyl-sulfonyl fluoride and 500 KIE/ml 'Trasylol'® proteinase-inhibitor (Bayer Leverkusen, Germany)] and centrifuged at 14000 rpm at 4°C for 15 min. Supernatant

protein was collected, and total protein concentration was determined using Bradford protein assay (Bio-Rad, Hercules, CA). Western blot analysis was performed as described in our previous study (20). Briefly, 50 µg of total protein was mixed with loading buffer, boiled for 5 min and separated by 15% polyacrylamide gel electrophoresis. Then protein was transferred onto a polyvinylidene difluoride membrane using a transblot apparatus. After blocking in 10% skim milk in 0.1% Tween-20 - Tris-Buffered Saline (TBS) with 0.1% Tween-20, the membrane filter was incubated overnight with the 1:100 diluted anti-Id1, -Id2 or -Id3 antibodies at 4˚C. The membranes were probed with 1:2000 diluted goat anti-rabbit coupled to horseradish peroxidase antibody (HRP; Dako, Denmark) for 1 h. The protein bands were visualized using an enhanced chemiluminescence (ECL) detection kit (Amersham, Buckinghamshire, UK), according to the instructions provided by the manufacturer. As a reference protein, actin was immunoblotted in the same protein extracts using rabbit anti-human actin polyclonal antibody (A-2066; Sigma, St. Louis, MO). The amount of actin in the protein extracts did not change (data not shown). The expressions of the proteins were evaluated by measuring optical densities of the protein bands, using NIH Image 1.61 software (National Institutes of Health; Bethesda, MD) and the expression value was calculated as compared to the actin band.

Immunohistochemistry. Formalin-fixed, paraffin-embedded liver tissues were sliced (4-µm thick), placed on microscope glass slides and subjected to immunostaining using an Avidin Biotin Complex (ABC) technique, as described previously (21). Where indicated, immunostaining for all three Id proteins was performed on serial sections. In brief, the sections were deparaffinized in xylene, rehydrated, boiled in antigen retrieval buffer (21) and washed with water. They were then treated with 1% hydrogen peroxide in methanol for 20 min to inhibit endogenous peroxidase. After incubation with 10% normal goat serum for 20 min to block non-specific binding, the sections were incubated for 16 h at 4˚C with one of the indicated primary antibodies. The antibodies to Id1 and Id3 were used at a concentration of 4 µg/ml, and the antibody to Id2 was used at 2 µg/ml. Detection of bound antibodies was performed using the peroxidase from the Dako EnVision+™ Systems kit (Dako, Carpinteria, CA) according to the instructions supplied by the manufacturer. Between incubations, sections were washed several times with phosphate-buffered saline. The peroxidase reaction was visualized by applying 0.02% 3,3'-diaminobenzidine tetrahydrochloride in 0.05 M Tris-buffer (pH 7.6) with 0.005% hydrogen peroxide for 2 min. The sections were then counterstained with Mayer's hematoxylin, dehydrated, cleared and mounted.

For negative controls, TBS was used as a substitute for the primary antibody to verify the possibility of false positive responses from the secondary antibody, and no staining was observed. For positive controls, sections of breast cancer expressing Id1 protein (14), and sections of pancreatic cancer expressing Id2 or Id3 protein (12) were included in the respective staining procedures (respectively shown on Fig. 1A, D and G). The positive controls displayed moderate cytoplasmic staining in each respective Id immunohistochemical staining. In addition, pre-absorbed antibodies with an excess amount of Id1-, Id2- or Id3-specific blocking peptides, completely abolished immunostaining on the sections of the respective primary antibody (Fig. 1C, F and I).

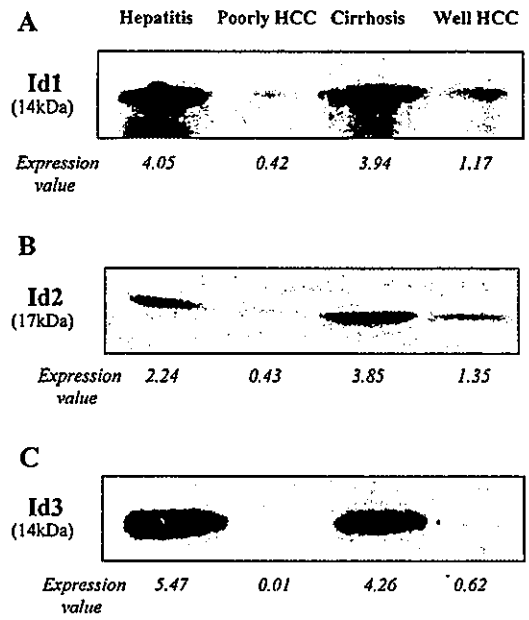

Figure 2. Western blot analysis for Id proteins. Two paired non-tumor liver and HCC tissues were examined for Id1 (A), Id2 (B) and Id3 (C) protein expression. The non-tumor tissues with cirrhosis and chronic hepatitis expressed clear bands for all Id proteins. The well-differentiated HCC expressed Id1 and Id2 at a modest level (A and B) and a faint signal was detected for Id3 (C), but the poorly-differentiated HCC did not express Id3 (C) or a slight band appeared for Id1 and Id2 (A and B). The expression value of Id protein band to actin band was analyzed densitometrically (lower panel). When pre-absorbed antibodies (by respective blocking peptides) were applied to the transferred membrane, no bands appeared on the blots (data not shown).

Evaluation of Id immunostaining. The intensity of the immunohistochemical signal was scored using a four-scale system: where 0 represented no immunoreactivity; 1, weak immunoreactivity; 2, moderate immunoreactivity and 3, strong immunoreactivity. The immunoreactivities in the positive controls were used as intensity score 2 (Fig. 1A, D and G). In correlation of Id protein immunoreactivity with clinicopathological characteristics and survival, the staining intensities were summarized, with intensity 0 and 1 labeled as 'low expression', the intensity 2 and 3 as 'high expression'.

All slides were interpreted in a blinded manner without knowledge of the clinical and pathological parameters by one of the investigators (B. Damdinsuren) and the final evaluation was cooperatively determined using a multi-head microscope by two investigators (B. Damdinsuren and M. Kondo).

Correlation of Id protein immunoreactivity with clinicopathological characteristics and survival. The clinicopathological features of 45 HCC patients with a histopathological diagnosis were examined. The parameters included age, gender, serum α-fetoprotein (AFP) level, tumor size, staging by the Japanese classification (22), histopathological grade of

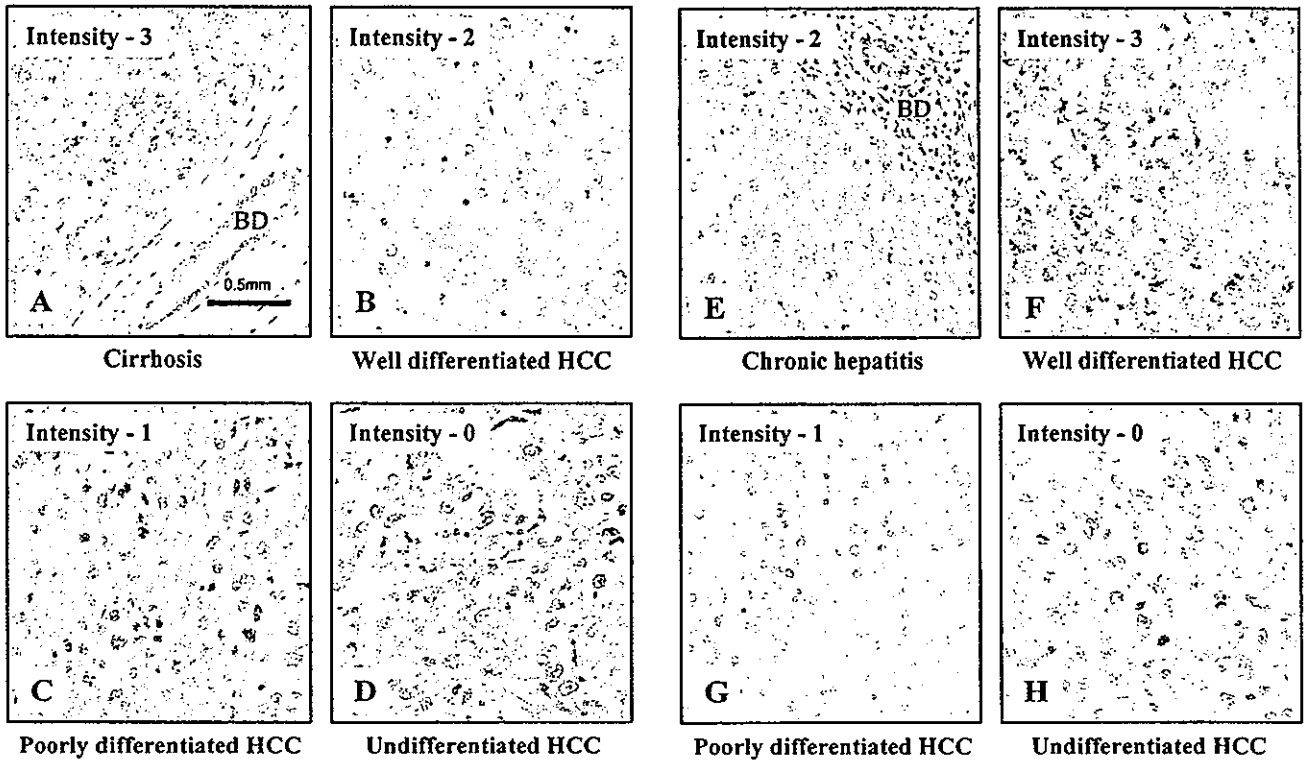

Figure 3. Immunohistochemical analysis of Id1 (A-D), Id2 (E-H) and Id3 (I-L) proteins in HCC and non-cancerous liver tissues. Representative samples of non-tumor liver and grades of tumor differentiation are shown with respective staining intensities. (A), Id1 expression in liver cirrhosis (intensity-3) with bile duct; (B), Well-differentiated (intensity-2); (C), Poorly-differentiated (intensity-1) and (D), Undifferentiated HCCs (intensity-0). (E), Id2 immunoreactivity in chronic hepatitis (intensity-2) with bile duct; (F), Well-differentiated (intensity-3); (G), Poorly-differentiated (intensity-1) and (H), Undifferentiated HCCs (intensity-0). (I), Id3 immunostaining in chronic hepatitis (intensity-3) with bile duct; (J), Well-differentiated (intensity-2); (K), Poorly-differentiated HCC (intensity-1) with adjacent liver cirrhosis (intensity-3) and (L), Undifferentiated HCC (intensity-0). The lymphocytes infiltrating the liver expressed strong immuno-reactivity for Id3 (arrowed on I and K). (Original magnification x400). BD, bile duct.

differentiation, presence of portal vein tumor thrombus, intrahepatic metastasis, septal formation, capsular formation and invasion. The histopathological diagnosis of tumor and non-tumor tissues was made by a histopathologist (K. Wakasa), who was blinded to the clinical background.

Disease-free survival (DFS) data were analyzed for 44 patients, who had undergone curative surgery and could be followed-up. They were followed for a period of 1-96 months (mean, 22.3 months) by tumor markers (serum AFP or PIVKA-II) and/or imaging modalities. DFS time was defined from the date of surgery to the date of tumor recurrence. The postoperative DFS curves were constructed by the Kaplan-Meier method.

Statistical analyses. Statistical analyses were performed using the StatView J-5.0 program (Abacus Concepts Inc., Berkeley, CA). The χ^2 and Fisher's exact tests were employed for analysis of the association between Id expression and clinicopathological parameters. DFS and its statistical significance were analyzed by the log-rank test. In all analyses, $p<0.05$ were considered statistically significant.

Results

Western blot analysis for Id proteins. To confirm the specificity of Id1, Id2 and Id3 antibodies and check the expression level of Id proteins, a small set of tissue samples (two paired tumor and non-tumor liver tissues) was subjected to Western blot analysis (Fig. 2). The non-tumor tissues of chronic hepatitis

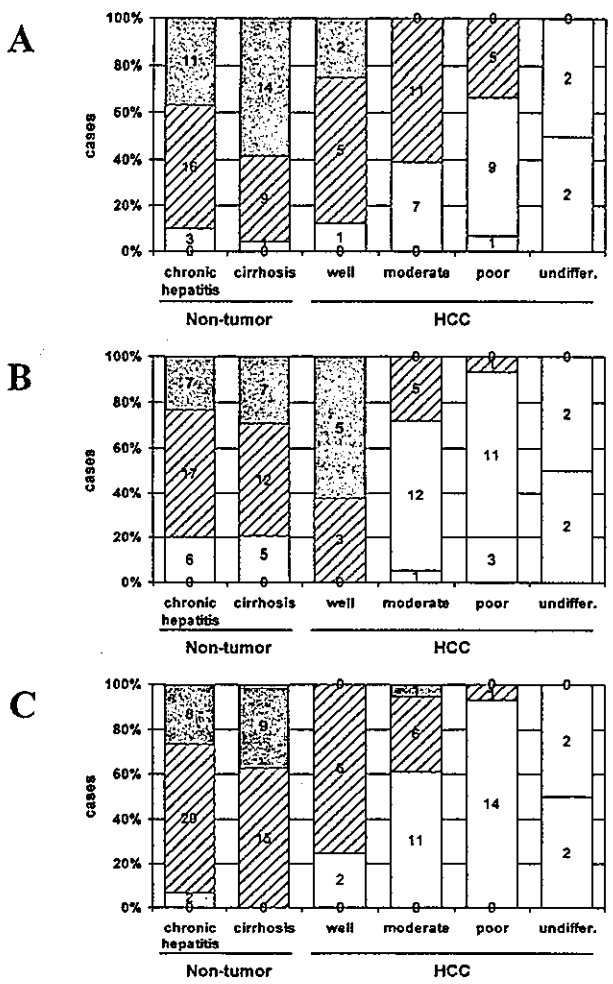

Figure 4. Distribution of the Id1, Id2 and Id3 expression in each histopathological groups of HCC and non-cancerous liver. Grey, strong immunostaining (intensity-3); Hatched, moderate immunostaining (intensity-2); Dotted, weak immunostaining (intensity-1); White, no immunostaining (intensity-0). All samples of non-tumor livers expressed the Ids. On the other hand, none of poorly and undifferentiated HCCs exhibited the strong Id immunostaining. The strong expression of Id1, 2 and 3 proteins increased from chronic hepatitis to cirrhosis. In HCC, Id protein expression was generally suppressed. The proportion of the samples with expression intensity-1 and -0 increased with tumor dedifferentiation and were frequently observed in poorly or undifferentiated HCCs. The number on the bars means the number of the cases with respective immunointensity.

or liver cirrhosis expressed clear bands for all Id proteins, while well-differentiated HCC expressed Id1 and Id2 proteins at a moderate level and Id3 protein to a lesser extent (lower panel). In contrast, Id1 and Id2 protein expression was weak or the Id3 protein expression was not detected in a poorly-differentiated HCC. When pre-absorbed antibodies (with respective blocking peptides) were applied to the transferred membrane instead of the Id antibodies, no bands appeared on the blots (data not shown). The results of immunostaining were in agreement with those obtained by Western blot analysis in each sample.

Immunohistochemistry. Localization and expression levels of Id1, Id2 and Id3 proteins were investigated by immunohistochemistry in liver tissues from 54 patients with HCC. These exhibited cytoplasmic immunostaining for all Id proteins. Fig. 3 illustrates typical staining for Id proteins and corresponding intensity scores in the representative cancerous and non-cancerous liver tissues. Heterogeneous staining was observed in <10% slides in all Id proteins because of heterogeneous histology of HCC and the intensity was evaluated by the major staining part.

The non-cancerous liver tissues commonly displayed strong and moderate immunoreactivity of all Id proteins, which reached 93% (25 and 25 cases), 80% (14 and 29 cases) and 96% (17 and 35 cases) of the patients respectively for Id1, Id2 and Id3 (Fig. 4). Sample without Id expression was not found among the non-tumor livers. The proportion of cases with strong expression (intensity-3) of Id1, 2 and 3 increased from chronic hepatitis (n=30) to cirrhosis (n=24), respectively from 11 (37%) to 14 (58%), from 7 (23%) to 7 (29%) and from 8 (27%) to 9 (38%) cases. However, the difference in proportion of cases expressing a high level of Id1, 2 and 3 between chronic hepatitis and liver cirrhosis was not significant. In HCC tissues, Id protein expression was generally suppressed, as shown by the weak expression (intensity-1) of Id1, Id2 and Id3 in 42.2% (19 cases), 55.6% (25 cases) and 64.4% (29 cases), respectively of 45 patients. The expression pattern of Ids in HCCs was significantly decreased compared to non-tumor tissues ($p<0.0001$ for each Id protein). Furthermore, in 29 (64%) of the paired samples for Id1, in 32 (71%) for Id2 and in 35 (79%) for Id3, HCC tissue showed weaker Id immunoreactivity than adjacent non-tumor tissue. However, Id protein expression in HCC varied considerably depending on the histological differentiation (Figs. 3 and 4). Well-differentiated HCCs mostly exhibited strong or moderate immunostaining for all Id proteins (in 7, 8 and 6 of 8 cases for Id1, 2 and 3, respectively), while proportion of the samples with expression intensity-1 and -0 increased with tumor dedifferentiation and frequently observed in poorly (66.7, 93.3 and 93.3% respectively for Id1, 2 and 3) or undifferentiated (100% in all Ids) HCCs (Fig. 4).

Intrahepatic bile ducts and blood vessels were also stained for each Id protein, and showed a range of low to high expression (Fig. 3A, E and I). Strong immunoreactivity for Id3 was observed in lymphocytes, which were crowded in the non-tumor side near the tumor margin and infiltrated into the tumor tissue (Fig. 3I and K, indicated by arrows).

Correlation between Id protein expression and clinicopathological features. To evaluate the role of Id proteins in tumor progression, we examined the correlations between expression of each Id protein and various clinicopathological features of the HCCs (Table I).

Expression levels of all Id proteins correlated with HCC differentiation ($p=0.004$, 0.001 and 0.001) and absence of portal vein tumor thrombosis ($p=0.002$, <0.001 and 0.037, respectively, for Id1, 2 and 3). Id1 expression also correlated inversely with tumor size ($p=0.01$), stage ($p=0.02$) and presence of intrahepatic metastasis ($p<0.001$). Id2 expression correlated inversely with HCC size ($p=0.035$) and presence of intrahepatic metastasis ($p=0.047$). Id3 immunoreactivity was significantly down-regulated in tumors with capsular formation ($p=0.023$).

Table I. Relationship between Id expressions and clinicopathological parameters in 45 cases with HCC[a].

	Id1		Id2		Id3	
	Low	High	Low	High	Low	High
Age						
≤60 years	13	9	18	4	15	7
>60 years	9	14	13	10	16	7
Gender						
Male	18	20	25	13	26	12
Female	4	3	6	1	5	2
Tumor size						
≤2 cm	3	9	6	6	5	7
2-5 cm	7	11 [c]	11	7 [c]	14	4
>5 cm	12	3	14	1	12	3
Histology grade						
Well and moderate	8	18 [c]	13	13 [c]	13	13 [c]
Poor and undifferentiated	14	5	18	1	18	1
Portal vein tumor thrombus						
No	7	18 [c]	12	13 [c]	14	11 [c]
Yes	15	5	19	1	17	3
Intrahepatic metastasis						
No	11	22 [c]	20	13 [c]	21	12
Yes	11	1	11	1	10	2
Septal formation						
No	9	10	14	5	12	7
Yes	13	13	17	9	19	7
Capsular formation						
No	6	9	8	7	7	8 [c]
Yes	16	14	23	7	24	6
Capsular invation						
No	5	6	8	3	9	2
Yes	11	8	15	4	15	4
Tumor stage[b]						
I and II	11	19 [c]	20	10	19	11
III and IV	11	4	11	4	12	3
α-fetoprotein						
≤5 ng/ml	6	8	10	4	9	5
>5 ng/ml	16	15	21	10	22	9

[a]p-value was calculated by χ^2 test. [b]Japanese classification (22). [c]Statistically significant, $p<0.05$.

Prognostic significance of Id proteins. We investigated the prognostic value of each Id protein in 44 patients who underwent curative surgery, analyzing the DFS rate by the Kaplan-Meier method and log-rank test (Fig. 5). Patients with low Id1 expression had a significantly shorter DFS time than those with high expression (p=0.047). A similar tendency was also observed with Id2 and Id3 proteins, but statistical significance was not observed. Multivariate analysis using the Cox regression model showed that none of Id protein expressions was a significant covariate with DFS (data not shown).

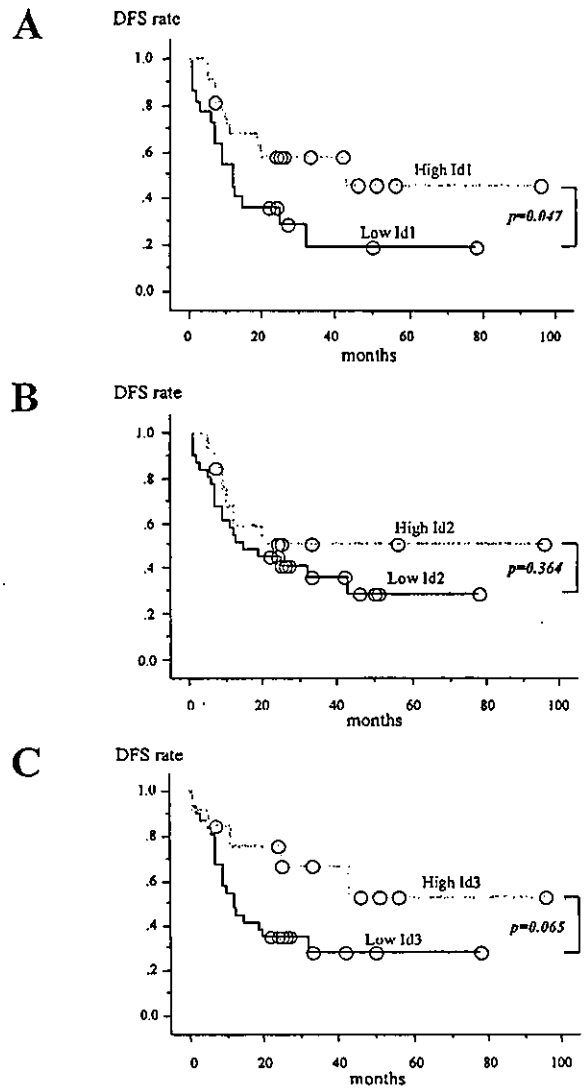

Figure 5. Kaplan-Meier curves for disease-free survival (DFS) of patients with high and low Id1 (A), Id2 (B) and Id3 (C) expression. Low expression of Id1 protein in HCC was significantly associated with shorter DFS (p=0.047). The mean follow-up period for patient prognosis was 22.3 months.

Discussion

The present study was performed in an effort to examine the expression of Id proteins (Id1-3) in human HCC and to address the relationship between their expression and clinicopathological features.

HCC and non-tumor liver tissues showed cytoplasmic immunostaining for all Id proteins, similar to pancreatic and breast cancers (12,14). In present study, the expression of all Id proteins was down-regulated in HCCs and significantly decreased in less differentiated tumors (Table I, Figs. 3 and 4). The results from correlation of Id expression in HCC with clinicopathological features indicated that the expression of Id proteins was associated with a non-aggressive phenotype of HCC, including correlation with smaller size (Id1, Id2), early stage (Id1), absence of portal vein tumor thrombus (Id1, Id2, Id3), intrahepatic metastasis (Id1, Id2) and capsular formation (Id3) (Table I). Consistent with these findings, patients with high Id1 expression had significantly longer DFS time compared with the low Id1 expression group (Fig. 5).

Generally, Id proteins have been shown to function as negative regulator of differentiation (9,10), with exception of positive regulation, described in myeloid cells, astrocytes and adipocytes (23-25). In human cancers, expression of Ids was correlated with tumor progression and aggressive phenotype of breast, colorectal, pancreatic, prostate and ovarian cancers (12-16). However, our study revealed opposite finding for HCC (Table I, Figs. 4 and 5), and comparable data were exposed by gene expression profiling analysis, with down-regulation of *Id1* from well- to moderately-differentiated HCCs (26). The reason of the difference in expression of Ids between HCC and the other cancers remains unclear, however, involvement of transforming growth factor ß (TGF-ß) in hepatocarcinogenesis might provide a clue to explain this difference. Recent findings in Id upstream signaling mechanisms revealed that *Ids* are direct TGF-ß1 target gene whose expression can be inhibited through activation of Smad3-ATP pathway, specifically in epithelial cells (11,27,28). Interestingly, many investigators demonstrated that non-tumor livers lacked the TGF-ß1, however HCC showed intense expression and that was increased in less differentiated tumors (29,30). Idobe *et al* showed that in 70% of the cases the TGF-ß1 was overexpressed in HCCs compared to non-tumor liver, which concur with our findings that in 64-79% of patients Ids were decreased in the tumor (30). Expression of TGF-ß1 in breast, prostate, pancreas and ovarian cancers has been reported to correlate with longer survival, as well as with low grade of malignancy (28,31-34). Although in colorectal cancers the expression of TGF-ß1 was increased, the signaling was interrupted with down-regulation of TGF-ß receptor (35). These findings in diverse expression of TGF-ß1 in HCC and in the other tumors may explain partly the different expression patterns of Id through its inhibition by TGF-ß1.

In the present study, clinicopathological survey demonstrated a significant correlation between Id proteins expression and differentiation of carcinoma. It is known that small HCCs increase in size and become less differentiated, the number of portal tracts apparently decreases and intra-tumoral arterioles develop (36-38). In pathological conditions, endotoxins and pro-inflammatory cytokines, such as tumor necrosis factor α, in portal blood flow might affect hepatic cells (39). This substance has been shown to induce Id protein expression (40). Thus, we speculate that early HCC, which usually presents well-differentiated histology with few arterial tumor vessels and contains pre-existing portal tracts, might be influenced by these Id inducers via the portal blood flow, resulting in high expression of Ids in well-differentiated HCC. On the other hand, advanced HCC might be less influenced due to main blood supply by arterial flow and lack of the portal tracts.

Recently, Ouyang *et al* reported that Id1 protein was increased during prostate carcinogenesis (41). From the pathological perspective, it has been shown that HCC develops as a tumor with a well-differentiated histology on the background of liver cirrhosis and chronic hepatitis, and progresses to less differentiated morphology (1,42,43). In our

present study, the proportion of strongly Id expressing cases increased from chronic hepatitis to cirrhosis (Fig. 4). Furthermore, frequent higher expression of Id proteins was observed in small size and well-differentiated HCCs with decreases of Ids in less-differentiated tumors (Table I, Figs. 4 and 5). These results revealed that Ids were involved in the early stage of hepatocarcinogenesis. Finally, our data suggested the possible strategy for prevention, as well as in treatment of human HCC, through targeting Id expression by use of antisense constructs as described previously for breast cancer therapy (44).

In conclusion, the present study demonstrated that Id1, 2 and 3 might play a role in the early stages of hepatocarcinogenesis, but not in the development of advanced carcinoma, and might consequently be related to HCC dedifferentiation.

Acknowledgements

This work was supported by Grant-in-Aid for Scientific Research provided by the Ministry of Education, Culture, Sports, Science and Technology, Japan.

References

1. Llovet JM, Burroughs A and Bruix J: Hepatocellular carcinoma. Lancet 362: 1907-1917, 2003.
2. Befeler AS and Di Bisceglie AM: Hepatocellular carcinoma: diagnosis and treatment. Gastroenterology 122: 1609-1619, 2002.
3. Massari ME and Murre C: Helix-loop-helix proteins: regulators of transcription in eucaryotic organisms. Mol Cell Biol 20: 429-440, 2000.
4. Benezra R, Devis RL, Lockshon D, Turner DL and Weintraub H: The protein Id: a negative regulator of helix-loop-helix DNA binding proteins. Cell 61: 49-59, 1990.
5. Hara E, Yamaguchi T, Nojima H, Ide T, Campisi J, Okayama H and Oda K: Id-related genes encoding helix-loop-helix proteins are required for G1 progression and are repressed in senescent human fibroblasts. J Biol Chem 269: 2139-2145, 1994.
6. Biggs J, Murphy EV and Israel MA: Id-like helix-loop-helix protein expressed during early development. Proc Natl Acad Sci USA 89: 1512-1516, 1992.
7. Ellmeier W, Aguzzi A, Kleiner E, Kurzbauer R and Weith A: Mutually exclusive expression of a helix-loop-helix gene and N-myc in human neuroblastomas and in normal development. EMBO J 11: 2563-2571, 1992.
8. Pagliuca A, Bartoli PC, Saccone S, Della Valle G and Lania L: Molecular cloning of ID4, a novel dominant negative helix-loop-helix human gene on chromosome 6p21.3-p22. Genomics 27: 200-203, 1995.
9. Norton JD: Id helix-loop-helix proteins in cell growth, differentiation and tumorigenesis. J Cell Science 113: 3897-3905, 2000.
10. Israel MA, Hernandez MC, Florio M, Andres-Barquin PJ, Mantani A, Carter JH and Julin CM: Id gene expression as a key mediator of tumor cell biology. Cancer Res 59: 1726S-1730S, 1999.
11. Ruzinova MB and Benezra R: Id proteins in development, cell cycle and cancer. Trends Cell Biol 13: 410-418, 2003.
12. Maruyama H, Kleeff J, Wildi S, Friess H, Buchler MW, Israel MA and Korc M: Id-1 and Id-2 are overexpressed in pancreatic cancer and in dysplastic lesions in chronic pancreatitis. Am J Path 155: 815-822, 1999.
13. Wilson JW, Deed RW, Inoue T, Balzi M, Becciolini A, Faraoni P, Potten CS and Norton JD: Expression of Id Helix-Loop-Helix proteins in colorectal adenocarcinoma correlates with p53 expression and mitotic index. Cancer Res 61: 8803-8810, 2001.
14. Lin CQ, Singh J, Murata K, Itahana Y, Parrinello S, Liang SH, Gillett CE, Campisi J and Desprez PY: A role for Id-1 in the aggressive phenotype and steroid hormone response of human breast cancer cells. Cancer Res 60: 1332-1340, 2000.
15. Schindl M, Schoppmann SF, Strobel T, Heinzl H, Leisser C, Horvat R and Birner P: Level of Id-1 protein expression correlates with poor differentiation, enhanced malignant potential and more aggressive clinical behavior of epithelial ovarian tumors. Clin Cancer Res 9: 779-785, 2003.
16. Ouyang XS, Wang X, Lee DT, Tsao SW and Wong YC: Overexpression of ID-1 in prostate cancer. J Urol 167: 2598-2602, 2002.
17. Lyden D, Young AZ, Zagzag D, Yan W, Gerald W, O'Reilly R, Bader BL, Hynes RO, Zhuang Y, Manova K and Benezra R: Id1 and Id3 are required for neurogenesis, angiogenesis and vascularization of tumour xenografts. Nature 401: 670-677, 1999.
18. Langlands K, Down GA and Kealey T: Id proteins are dynamically expressed in normal epidermis and dysregulated in squamous cell carcinoma. Cancer Res 60: 5929-5933, 2000.
19. Lee TK, Man K, Ling MT, Wang XH, Wong YC, Lo CM, Poon RT, Ng IO and Fan ST: Overexpression of Id-1 induces cell proliferation in hepatocellular carcinoma through inactivation of p16INK4a/RB pathway. Carcinogenesis 24: 1729-1736, 2003.
20. Yamamoto H, Kondo M, Nakamori S, Nagano H, Wakasa K, Sugita Y, Chang-De J, Kobayashi S, Damdinsuren B, Dono K, Umeshita K, Sekimoto M, Sakon M, Matsuura N and Monden M: JTE-522, a cyclooxygenase-2 inhibitor, is an effective chemopreventive agent against rat experimental liver fibrosis. Gastroenterology 125: 556-571, 2003.
21. Ciaparrone M, Yamamoto H, Yao Y, Sgambato A, Cattoretti G, Tomita N, Monden T, Rotterdam H and Weinstein IB: Localization and expression of p27KIP1 in multistage colorectal carcinogenesis. Cancer Res 58: 114-122, 1998.
22. Liver Cancer Study Group of Japan (eds). General rules for the clinical and pathological study of primary liver cancer. 2nd English edition. Kanehara & Co., Ltd., Tokyo, p23, 2003.
23. Ishiguro A, Spirin KS, Shiohara M, Tobler A, Gombart AF, Israel MA, Norton JD and Koeffler HP: Id2 expression increases with differentiation of human myeloid cells. Blood 87: 5225-5231, 1996.
24. Andres-Barquin PJ, Hernandez MC, Hayes TE, McKay RD and Israel MA: Id genes encoding inhibitors of transcription are expressed during *in vitro* astrocyte differentiation and in cell lines derived from astrocytic tumors. Cancer Res 57: 215-220, 1997.
25. Chen H, Weng YC, Schatteman GC, Sanders L, Christy RJ and Christy BA: Expression of the dominant-negative regulator Id4 is induced during adipocyte differentiation. Biochem Biophys Res Commun 256: 614-619, 1999.
26. Midorikawa Y, Tsutsumi S, Taniguchi H, Ishii M, Kobune Y, Kodama T, Makuuchi M and Aburatani H: Identification of genes associated with dedifferentiation of hepatocellular carcinoma with expression profiling analysis. Jpn J Cancer Res 93: 636-643, 2002.
27. Kang Y, Chen CR and Massague J: A self-enabling TGF beta response coupled to stress signaling: Smad engages stress response factor ATF3 for Id1 repression in epithelial cells. Mol Cell 11: 915-926, 2003.
28. Ling MT, Wang X, Tsao SW and Wong YC: Down-regulation of Id-1 expression is associated with TGF beta 1-induced growth arrest in prostate epithelial cells. Biochim Biophys Acta 1570: 145-152, 2002.
29. Bedossa P, Peltier E, Terris B, Franco D and Poynard T: Transforming growth factor-beta 1 (TGF-beta 1) and TGF-beta 1 receptors in normal, cirrhotic and neoplastic human livers. Hepatology 21: 760-766, 1995.
30. Idobe Y, Murawaki Y, Kitamura Y and Kawasaki H: Expression of transforming growth factor-beta 1 in hepatocellular carcinoma in comparison with the non-tumor tissue. Hepatogastroenterology 50: 54-59, 2003.
31. Pilichowska M, Kimura N, Fujiwara H and Nagura H: Immunohistochemical study of TGF-alpha, TGF-beta1, EGFR and IGF-1 expression in human breast carcinoma. Mod Pathol 10: 969-975, 1997.
32. Mizukami Y, Nonomura A, Yamada T, Kurumaya H, Hayashi M, Koyasaki N, Taniya T, Noguchi M, Nakamura S and Matsubara F: Immunohistochemical demonstration of growth factors, TGF-alpha, TGF-beta, IGF-I and neu oncogene product in benign and malignant human breast tissues. Anticancer Res 10: 1115-1126, 1990.
33. Coppola D, Lu L, Fruehauf JP, Kyshtoobayeva A, Karl RC, Nicosia SV and Yeatman TJ: Analysis of p53, p21WAF1 and TGF-beta1 in human ductal adenocarcinoma of the pancreas: TGF-beta1 protein expression predicts longer survival. Am J Clin Pathol 110: 16-23, 1998.

34. Henriksen R, Gobl A, Wilander E, Oberg K, Miyazono K and Funa K: Expression and prognostic significance of TGF-beta isotypes, latent TGF-beta 1 binding protein, TGF-beta type I and type II receptors, and endoglin in normal ovary and ovarian neoplasms. Lab Invest 73: 213-220, 1995.
35. Matsushita M, Matsuzaki K, Date M, Watanabe T, Shibano K, Nakagawa T, Yanagitani S, Amoh Y, Takemoto H, Ogata N, Yamamoto C, Kubota Y, Seki T, Inokuchi H, Nishizawa M, Takada H, Sawamura T, Okamura A and Inoue K: Down-regulation of TGF-beta receptors in human colorectal cancer: implications for cancer development. Br J Cancer 80: 194-205, 1999.
36. Winter TC III, Takayasu K, Muramatsu Y, Furukawa H, Wakao F, Koga H, Sakamoto M, Hirohashi S and Freeny PC: Early advanced hepatocellular carcinoma: evaluation of CT and MR appearance with pathologic correlation. Radiology 192: 379-387, 1994.
37. Ueda K, Terada T, Nakanuma Y and Matsui O: Vascular supply in adenomatous hyperplasia of the liver and hepatocellular carcinoma: a morphometric study. Hum Pathol 23: 619-626, 1992.
38. Nakashima Y, Nakashima O, Hsia CC, Kojiro M and Tabor E: Vascularization of small hepatocellular carcinomas: correlation with differentiation. Liver 19: 12-18, 1999.
39. Crawford JM: Cellular and molecular biology of the inflamed liver. Curr Opin Gastroenterol 13: 175-185, 1997.
40. Tzeng SF, Kahn M, Liva S and De Vellis J: Tumor necrosis factor-alpha regulation of the Id gene family in astrocytes and microglia during CNS inflammatory injury. Glia 26: 139-152, 1999.
41. Ouyang XS, Wang X, Lee DT, Tsao SW and Wong YC: Up-regulation of TRPM-2, MMP-7 and ID-1 during sex hormone-induced prostate carcinogenesis in the Noble rat. Carcinogenesis 22: 965-973, 2001.
42. Sugihara S, Nakashima O, Kojiro M, Majima Y, Tanaka M and Tanikawa K: The morphologic transition in hepatocellular carcinoma. A comparison of the individual histologic features disclosed by ultrasound-guided fine-needle biopsy with those of autopsy. Cancer 70: 1488-1492, 1992.
43. Nakashima O, Sugihara S, Kage M and Kojiro M: Pathomorphologic characteristics of small hepatocellular carcinoma: a special reference to small hepatocellular carcinoma with indistinct margins. Hepatology 22: 101-105, 1995.
44. Fong S, Itahana Y, Sumida T, Singh J, Coppe JP, Liu Y, Richards PC, Bennington JL, Lee NM, Debs RJ and Desprez PY: Id-1 as a molecular target in therapy for breast cancer cell invasion and metastasis. Proc Natl Acad Sci USA 100: 13543-13548, 2003.

Combination of IFN-α and 5-Fluorouracil Induces Apoptosis through IFN-α/β Receptor in Human Hepatocellular Carcinoma Cells

Motoi Kondo, Hiroaki Nagano, Hiroshi Wada, Bazarragchaa Damdinsuren, Hirofumi Yamamoto, Nobuaki Hiraoka, Hidetoshi Eguchi, Atsushi Miyamoto, Tameyoshi Yamamoto, Hideo Ota, Masato Nakamura, Shigeru Marubashi, Keizo Dono, Koji Umeshita, Shoji Nakamori, Masato Sakon, and Morito Monden

Department of Surgery and Clinical Oncology, Graduate School of Medicine, Osaka University, Osaka, Japan

ABSTRACT

Purpose: **Several studies showed the effectiveness of combination therapy with IFN-α and 5-fluorouracil (5-FU) for advanced hepatocellular carcinoma. However, only little is known about the underlying mechanism of combination therapy. In the present study, we examined whether apoptosis through IFN-α/β receptor (IFN-α/βR) was associated with the effects of combination therapy.**

Experimental Design: **HuH7, PLC/PRF/5, HLE, and HLF were treated with IFN- (500 units/mL), 5-FU (0.5 μg/mL), or their combination for 10 days. In addition, *IFN-α/βR* gene transfer with combination therapy was done.**

Results: **Ten-day treatment by combination therapy resulted in >80% cell growth inhibition. Terminal deoxynucleotidyl transferase–mediated dUTP nick end labeling analysis showed synergistic effects for combination therapy on PLC/PRF/5, HLE, and HLF. Concordant results were obtained with DNA fragmentation. Moreover, there was an evidence showing that changes in the expression of Bcl-2 family lead to apoptosis. On the other hand, the expression of IFN-α/βR and up-regulation of α-phospho–signal transducer and activator of transcription 1, IFN regulatory factor-1 by combination therapy were observed in all cell lines. Furthermore, IFN-α/type 2 IFN receptor long form–transfected HuH7 cells treated with combination therapy showed strong DNA fragmentation compared with non-transfected or transfected with IFN-α- and 5-FU-treated HuH7.**

Conclusions: **Our results showed that combination of IFN-α plus 5-FU strongly induced cell growth inhibition of human hepatocellular carcinoma cells and indicated that one of the direct mechanisms of combination therapy may in part be attributable to alterations in induction of apoptosis through IFN-α/βR.**

INTRODUCTION

Hepatocellular carcinoma (HCC) is one of the most frequent malignancies in Southeast Asia and Africa. The prognosis of HCC is generally poor, and the 5-year survival rate is limited to 25% to 49% after surgery (1–3). In particular, growth of HCC with macroscopic tumor thrombi in the major branches of portal vein is extremely aggressive and almost terminal feature. In addition, conventional therapies, such as transcatheter arterial embolization, percutaneous ethanol injection therapy, and microwave coagulation therapy, are not generally indicated for such advanced HCC due to low efficacy and potential complications (4, 5). Most HCC patients with these thrombi often develop tumor recurrence, and over half of them die within 1 year after surgery even if curative resection is done (6). The prognosis of patients with unresectable HCC with portal tumor thrombi is much worse, and most patients die within several months after the diagnosis (6). Therefore, effective therapeutic strategy for advanced HCC is desirable.

We have already reported a patient with recurrent HCC and multiple lung and bone metastases whose malignant condition was uncontrollable by conventional therapies but showed almost complete regression of the tumors following treatment with tegafur/uracil and IFN-α (7). The patient died 6 years after the initiation of this treatment. This surprise outcome let us systematically investigate the beneficial effects of the combination therapy of an anticancer drug and IFN-α for advanced HCCs.

The combination therapy of IFN-α and 5-fluorouracil (5-FU) was initially proposed in 1988 based on *in vitro* experiments on colon cancer cells (8). Subsequently, this combination therapy was applied to various types of human carcinomas. In patients with colorectal carcinoma, esophageal carcinoma, or gastric carcinoma, satisfactory results were obtained (9–13). In our clinical studies, we observed outstanding effects with IFN-α and 5-FU therapy in patients with advanced HCC (14). Several *in vitro* studies have provided some explanations about the synergistic effects of the combination of IFN-α and 5-FU (15–18). However, there are a few studies that have examined the effects of combination therapy on fundamental cell biology in human HCC cells (19–21). Recently, our study showed that up-regulation of $p27^{Kip1}$ and the expression of

Received 5/13/04; revised 10/5/04; accepted 11/11/04.
Grant support: Aid for Cancer Research from the Ministry of Health and Welfare of Japan and Osaka Medical Research Foundation for Incurable Diseases award.
The costs of publication of this article were defrayed in part by the payment of page charges. This article must therefore be hereby marked *advertisement* in accordance with 18 U.S.C. Section 1734 solely to indicate this fact.
Requests for reprints: Hiroaki Nagano, Department of Surgery and Clinical Oncology, Graduate School of Medicine, Osaka University, 2-2 Yamada-oka E2, Suita, Osaka 565-0871, Japan. Phone: 81-6-6879-3251; Fax: 81-6-6879-3259; E-mail: hnagano@surg2.med.osaka-u.ac.jp.

IFN-α/β receptor (IFN-α/βR) were the direct mechanisms of combination therapy–mediated antitumor effects (19). These findings were further investigated in the present study.

In the present study, we examined the effects of combination therapy on apoptosis in four HCC cell lines. Moreover, we also examined the expression of IFN-α/βR and signal transduction because of IFN-α exerts its effect through the specific cell surface receptor.

MATERIALS AND METHODS

Reagents and Cell Lines. Purified human IFN-α was obtained from Otsuka Pharmaceutical Co. (Tokushima, Japan) and 5-FU was purchased from Kyowa Hakko Co. (Tokyo, Japan). Four human HCC cell lines, PLC/PRF/5, HuH7, HLE, and HLF, were purchased from the Japanese Cancer Research Resources Bank (Tokyo, Japan). They were maintained in DMEM supplemented with 10% fetal bovine serum at 37°C in a humidified incubator with 5% CO_2 in air. The following primary antibodies were used at appropriate concentrations as recommended by the manufacturer or used in previous studies: anti-human polyclonal IFN-α/βR antibody (Otsuka Pharmaceutical), anti-human monoclonal Bcl-x_L antibody (Transduction Laboratories, Lexington, KY), anti-human polyclonal Bax antibody (Lake Placid, NY), anti-human monoclonal Bcl-2 antibody (DAKO, Glostrup, Denmark), anti-human polyclonal α-phospho–signal transducer and activator of transcription 1 (STAT1) antibody (New England Biolabs, Inc., Beverly, MA), anti-human polyclonal IFN regulatory factor-1 (IRF-1) antibody (Santa Cruz Biotechnology, Santa Cruz, CA), and anti-human polyclonal actin antibody (Sigma, St. Louis, MO).

Use of IFN-α and/or 5-Fluorouracil at Various Concentrations for Growth Inhibition Assay and Induction of Apoptosis. These studies were done to examine whether IFN-α or 5-FU reduces the cell growth and induces apoptosis in a dose-dependent manner. Cells were added in 24-well dishes (4×10^3 per well for PLC/PRF/5 and 2×10^3 per well for HuH7, HLE, and HLF). The medium was replaced 24 hours later by 1 mL fresh medium containing various concentrations of IFN-α or 5-FU. The concentrations of IFN-α in growth inhibition assays for IFN-α alone were 50, 500, 5,000, and 25,000 units/mL and those of 5- FU were 0.05, 0.5, 5, and 10 μg/mL. HCC cells suspended in complete medium were used as a control for cell viability. The medium and drugs were changed every 48 hours. Ten days later, the number of viable cells was assessed using a hemocytometer by trypan blue dye exclusion.

To detect *in situ* apoptosis under same conditions of the growth inhibition assay, we applied terminal deoxynucleotidyl transferase–mediated dUTP nick end labeling (TUNEL) method using ApopTag kit (S7100, Oncor, Gaithersburg, MD) as described previously (22). This method can detect fragmented DNA ends of apoptotic cells. In this assay, free cells in the medium were harvested every 48 hours because some apoptotic cells did not attach to the dish during cell culture, whereas those attached to the dish were harvested 10 days later and then fixed with 10% buffered formaldehyde for detection of apoptotic cells. Terminal deoxynucleotidyl transferase was omitted from the nucleotide mixture for the negative control. As a positive control, we used paraffin-embedded sections of 10% buffered formalin-fixed rodent mammary glands (19). For quantification of apoptotic cells, 20 microscopic fields were randomly selected at ×200 magnification, >500 total cells were counted in each sample, and the percentage of apoptotic cells was calculated.

To investigate whether IFN-α and 5-FU have cooperative effects on cell growth inhibition and induction of apoptosis, growth inhibitory and TUNEL assays were done. Cells were exposed to IFN-α (50, 500, 5,000, and 25,000 units/mL) and 5-FU (0.05, 0.5, 5, and 10 μg/mL) for 10 days at various concentrations.

Dose Selection and Treatment Design in Mechanistic Study. In our clinical trial, the patients were treated with s.c. administration of IFN-α and intra-arterial infusion of 5-FU (14). IFN-α was administered on days 1, 3, and 5 of every week. Continuous infusion chemotherapy (5-FU) through the proper hepatic artery was done for 2 weeks via a catheter connected to a s.c. implanted drug delivery system (14). According to the clinical study, the concentration of 5-FU (0.5 μg/mL) was decided the same as that in plasma of patients treated by continuous infusion (23). In addition, the concentration of IFN-α was decided 500 units/mL because this concentration enhances the biochemical modulation of 5-FU in our earlier reports (19, 21).

To prepare a model similar to human therapy, the medium and drugs were changed every 48 hours and the effects were examined 10 days later because in human a clear effect of anticancer agents is not observed after a few days.

Growth Curves in Mechanistic Study. To examine whether IFN-α or 5-FU or their combination reduces the cell growth in a time-dependent manner, cells were uniformly seeded (4×10^3 per well for PLC/PRF/5 and 2×10^3 per well for HuH7, HLE, and HLF) in triplicates into 24-well dishes. Twenty-four hours later (day 0), the culture medium was removed and replaced with 1 mL fresh medium with or without IFN-α (500 units/mL) and 5-FU (0.5 μg/mL) as reported previously (19). The medium and drugs were changed every 48 hours. On days 2, 4, 6, 8, and 10, viable cells were counted using a hemocytometer by trypan blue dye exclusion.

Detection of Apoptosis in Mechanistic Study. To examine whether IFN-α or 5-FU or their combination induces the apoptosis in a time-dependent manner, we did TUNEL method using ApopTag kit to detect *in situ* apoptosis. Cells were uniformly seeded (4×10^4 per well for PLC/PRF/5 and 2×10^4 per well for HuH7, HLE, and HLF) into 10 cm diameter dishes and cultured for 10 days. The culture medium was replaced every 48 hours with 10 mL fresh medium with or without IFN-α (500 units/mL) and 5-FU (0.5 μg/mL). Cells free in the medium were harvested every 48 hours because some apoptotic cells did not attach to the dish during cell culture, whereas those attached to the dish were harvested 10 days later and then fixed with 10% buffered formaldehyde for detection of apoptotic cells. The apoptotic cell counts at days 4, 6, and 8 represented cumulative apoptotic cells detected during that particular 48-hour time period. Terminal deoxynucleotidyl transferase was omitted from the nucleotide mixture for the negative control. As a positive control, we used paraffin-embedded sections of 10% buffered formalin-fixed rodent mammary glands (19). For quantification of apoptotic cells, 20 microscopic fields were randomly selected at ×200 magnification, >500 total cells were counted in each sample, and the percentage of apoptotic cells was calculated.

DNA Fragmentation. Both floating and adherent HCC cells were harvested using the protocol described for the TUNEL method and washed with calcium- and magnesium-free PBS. DNA fragmentation was done according to the directions provided with the TACS ethidium bromide kit (Trevigen, Inc., Gaithersburg, MD). DNA (15 μg) samples were loaded onto a 1.5% agarose gel that was run at 130 V and then stained with 0.5 μg/mL ethidium bromide for 20 minutes. The stained gel was immersed in 5 μg/mL RNase A in H_2O overnight. DNA fragmentation was visualized under UV light.

Quantitative Real-time PCR by LightCycler for Detection of Cytochrome *c*. For detection of cytochrome *c*, the cells were incubatedwith medium alone or medium containing 500 units/mL IFN-α and/or 0.5 μg/mL 5-FU for 48 hours, and both floating and adherent cells were harvested. We examined the up-regulation of cytochrome *c* by restimulation with combination therapy using HuH7. In this protocol, on days 2, 4, 6, or 8, the cells were stimulated with 500 units/mL IFN-α and 0.5 μg/mL 5-FU, and both floating and adherent cells were harvested on days 4, 6, 8, and 10. Quantitative PCR was done using LightCycler (Idaho Technology, Idaho Falls, ID) as described previously by our laboratory (24–26). The PCR primers used for detection of cytochrome *c* cDNA were synthesized as reported previously (27). Briefly, 20 μL PCR reaction contained 0.25 μmol/L of each primer, LC-DNA Master SYBR Green I (Boehringer Mannheim, Mannheim, Germany), 2 mmol/L $MgCl_2$, and 2 μL cDNA as a template. PCR conditions for LightCycler were set up as follows: 1 cycle of denaturing at 95°C for 10 minutes followed by 40 cycles of 95°C for 15 seconds, 56°C for 10 seconds, and 72°C for 25 seconds. Fluorescence was acquired at the end of every 72°C extension phase.

Quantification data from each sample were analyzed using LightCycler analysis software. In this analysis, the background fluorescence was removed by setting a noise band. The transcription value of the target was obtained by plotting on a standard curve. The amount of each transcript was normalized according to that of glyceraldehyde-3-phosphate dehydrogenase quantified with the same sample. To distinguish the specific product from nonspecific products and primer dimers, melting curves of final PCR products were analyzed (28). Because different DNA products melt at different temperatures, it was possible to distinguish genuine products from primer dimers or nonspecific products (28).

Western Blot Analysis. For detection of apoptosis-related proteins, both floating and adherent cells were harvested as described for the TUNEL method and homogenized in 0.5 mL radioimmunoprecipitation assay buffer [25 mmol/L Tris (pH 7.4), 50 mmol/L NaCl, 0.5% sodium deoxycholate, 2% NP40, 0.2% SDS] containing protease inhibitors (1 mmol/L phenylmethylsulfonyl fluoride, 10 μg/mL aprotinin, and 10 μg/mL leupeptin). The homogenate was centrifuged at 14,000 rpm for 20 minutes at 4°C. The resulting supernatant was collected and total protein concentration was determined using the Bradford protein assay (Bio-Rad, Hercules, CA). Western blot analysis was done as described in our previous studies (29). Briefly, 100 μg of the total protein were premixed with loading buffer [0.05 mol/L Tris-HCl (pH 6.8), 2% SDS, 0.2 mol/L β-mercaptoethanol, 10% glycerol, 0.001% bromophenol blue], boiled for 5minutes, and subjected to SDS-PAGE on 10% gel. After electrophoresis, protein transfer was done onto a polyvinylidene difluoride membrane (Boehringer Mannheim) using a transblot apparatus in a buffer containing 0.02 mol/L Tris-HCl (pH 8.3), 0.2 mol/L glycine, and 20% methanol. After blocking in 10% skim milk, the membrane was incubated with the primary antibody, anti-Bax (dilution, 1:400), anti-Bcl-2 (1:300), anti-Bcl-x_L (1:1,000), or anti-actin (1:1,000), for 1 hour at room temperature. After three washes each for 5 minutes with TBS [0.02 mol/L Tris-HCl (pH 7.5), 0.1 mol/L NaCl] containing 0.2% Tween 20, the filter was incubated with the secondary antibody at a dilution of 1:2,000. The protein bands were detected using the enhanced chemiluminescence detection system (Amersham, Arlington Heights, IL) according to the instructions provided by the manufacturer.

For detection of α-phospho-STAT1 (1:400) and IRF-1 (1:200), the cells were incubated with medium alone or medium containing IFN-α (500 units/mL) and 5-FU (0.5 μg/mL) for 30 minutes and lysed in lysis buffer [50 mmol/L Tris (pH 7.5), 100 mmol/L NaCl, 50 mmol/L NaF, 3 mmol/L sodium orthovanadate, 1% Tween, proteinase inhibitors]. Concentrations were determined by the Bradford assay. For this assay, we used 12% SDS-PAGE and electroblotting onto a polyvinylidene difluoride membrane.

For detection of IFN-α/βR protein on the cell surface, subconfluent cells in 10 cm diameter dishes were used. HCC cells were minced and washed thrice with PBS (pH 7.5). Samples were soaked in 500 μL hypotonic buffer (1 mmol/L $NaHCO_3$) containing 2 mmol/L phenylmethylsulfonylfluoride and 1 μg/mL aprotinin for 30 minutes and centrifuged at 15,000 × *g* for 30 minutes. The pellet was mixed with 750 μL loading buffer [10% glycerol, 2% SDS, 62.5 mmol/L Tris-HCl (pH 6.8)] and centrifuged at 15,000 × *g* for 15 minutes to obtain the cell membrane fraction. An aliquot (50 μg of protein) of the cell membrane was subjected to immunoblotting as described previously (30) using IFN-α/βR antibody (1:60).

Transfection of IFN-α/βR. Full-length IFN-α/type 2 IFN receptor long form (IFNAR2c) plasmid was kindly obtained from Otsuka Pharmaceutical. Confluent HuH7 cells into six-well dish were used in this study. The cells were cultured with 1 mL fresh medium with 4 μg IFNAR2c plasmid, 250 μL Opti-MEM (Life Technologies, Gaithersburg, MD), 10 μL LipofectAMINE 2000 (Invitrogen Corp., San Diego, CA), and 250 μL Opti-MEM using the instructions provided by the manufacturer. The culture medium was removed 24 hours later and replaced with 1 mL fresh medium. For detection of IFNAR2c, adherent HCC cells were harvested 24 hours later. For detection of DNA fragmentation, the culture medium was removed 24 hours later and replaced with 1 mL fresh medium containing IFN-α, 5-FU, or IFN-α (500 units/mL) and 5-FU (0.5 μg/mL). Twenty-four hours later, DNA was isolated and analyzed as described above under DNA fragmentation.

Analysis of Cooperative Effects. Synergistic effect was examined by isobolographic analysis as described previously by our laboratory (19, 22). We used the equation: $D = [(Ac / Ae) + (Bc / Be)]$, where *A* and *B* are two drugs, *c* is the concentration of the agent used in the combination therapy, and *e* is the concentration of the agent used in monotherapy to exert the same effect of the combination therapy. When *D* was <0.8, the effect of the drugs used in the combination therapy was considered synergistic.

Statistical Analysis. Statistical analysis was done using the StatView J-5.0 program (Abacus Concepts, Inc., Berkeley, CA). Data are expressed as mean ± SE. Differences between groups were examined for statistical significance using Dunnett method and Student's t test. $P < 0.05$ denoted the presence of a statistically significant difference.

RESULTS

Growth Inhibition Assay and Induction of Apoptosis by Various Concentrations of IFN-α and/or 5-Fluorouracil. We tested the dose-dependent cell growth suppression of IFN-α or 5-FU treatment on four HCC cell lines. The growth of all cell lines were suppressed by IFN-α or 5-FU in a dose-dependent manner (Fig. 1*A* and *B*). IFN-α resulted in strong cell growth inhibition of PLC/PRF/5 but only relatively weak or moderate changes in HuH7, HLE, and HLF cells. 5-FU produced strong cell growth inhibition in HuH7 and relatively weak or moderate changes in PLC/PRF/5, HLE, and HLF. Furthermore, IFN-α-induced marked apoptosis of PLC/PRF/5 but relatively weak or moderate changes in HuH7, HLE, and HLF cells (Fig. 1*C*). 5-FU induced apoptosis in a dose-dependent manner in all cells (Fig. 1*D*).

To examine whether combination therapy have cooperative effects on cell growth inhibition and induction of apoptosis, cells were exposed to IFN-α and 5-FU for 10 days at various concentrations. Exposure of cells to a combination of IFN-α and 5-FU suppressed cell growth and increased apoptosis in all cell lines in a dose-dependent manner (Fig. 2). The experiments were repeated 10 times and the results were reproducible.

Combination Therapy Reduces Cell Growth of Hepatocellular Carcinoma Cells in a Time-Dependent Manner. The effects of each drug and combination therapy were examined over a 10-day period (Fig. 3). The cell growth of each cell line under combination therapy on day 10 was significantly lower than that under IFN-α or 5-FU alone ($P < 0.05$). In addition, the cell growth of each cell line treated with 5-FU on day 10 was significantly lower than the control and IFN-α ($P < 0.05$). The suppression rates of cell growth under combination therapy on day 10 for HuH7, PLC/PRF/5, HLE, and HLF were 89.7%, 90.9%, 90.2%, and 90.5%, respectively. Isobolographic analysis indicated that these cooperative effects in PLC/PRF/5, HLE, and HLF, but not in HuH7, cells were synergistic. The experiments were repeated 10 times for analysis and the results were reproducible.

Combination Therapy Induces Apoptosis of Hepatocellular Carcinoma Cells in a Time-Dependent Manner. To examine the combined effect of IFN-α and 5-FU on apoptosis, TUNEL assays were done 10 days after treatment (Fig. 4). The percentages of apoptotic cells of HuH7, PLC/PRF/5, HLE, and HLF at day 10 of combination treatment were 6.01 ± 0.21%, 9.91 ± 0.41%, 7.12 ± 0.25%, and 7.61 ± 0.11%, respectively. The numbers of apoptotic cells of each cell line on day 10 of combination therapy were significantly higher than IFN-α- and 5-FU-treated cells ($P < 0.05$), although no difference was observed between the latter groups. Isobolographic analysis indicated that the cooperative effects of combination therapy on apoptosis of PLC/PRF/5, HLE, and HLF were synergistic, excluding HuH7. The experiments were repeated 10 times for analysis and the results were reproducible.

Combination Therapy Induces DNA Fragmentation. All four HCC cells treated with IFN-α (500 units/mL) and 5-FU

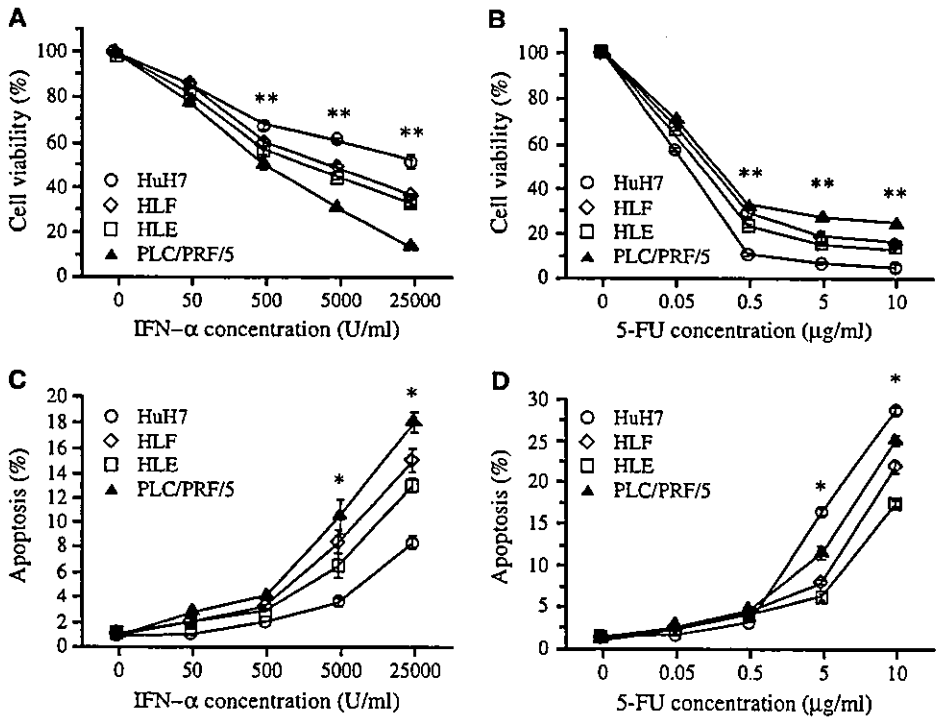

Fig. 1 Growth inhibitory effects and incidence of apoptosis with various concentrations of IFN-α (*A* and *C*) or 5-FU (*B* and *D*) on HCC cell lines. Cells were incubated for 10 days, and cell growth and apoptosis were determined as described in Materials and Methods. When IFN-α or 5-FU administered simultaneously, the antiproliferative effects and induction of apoptosis were dose dependent. Mean (*points*) ± SE (*bars*). *, $P < 0.05$, compared with each group; **, $P < 0.05$, compared with PLC/PRF/5 and HuH7.

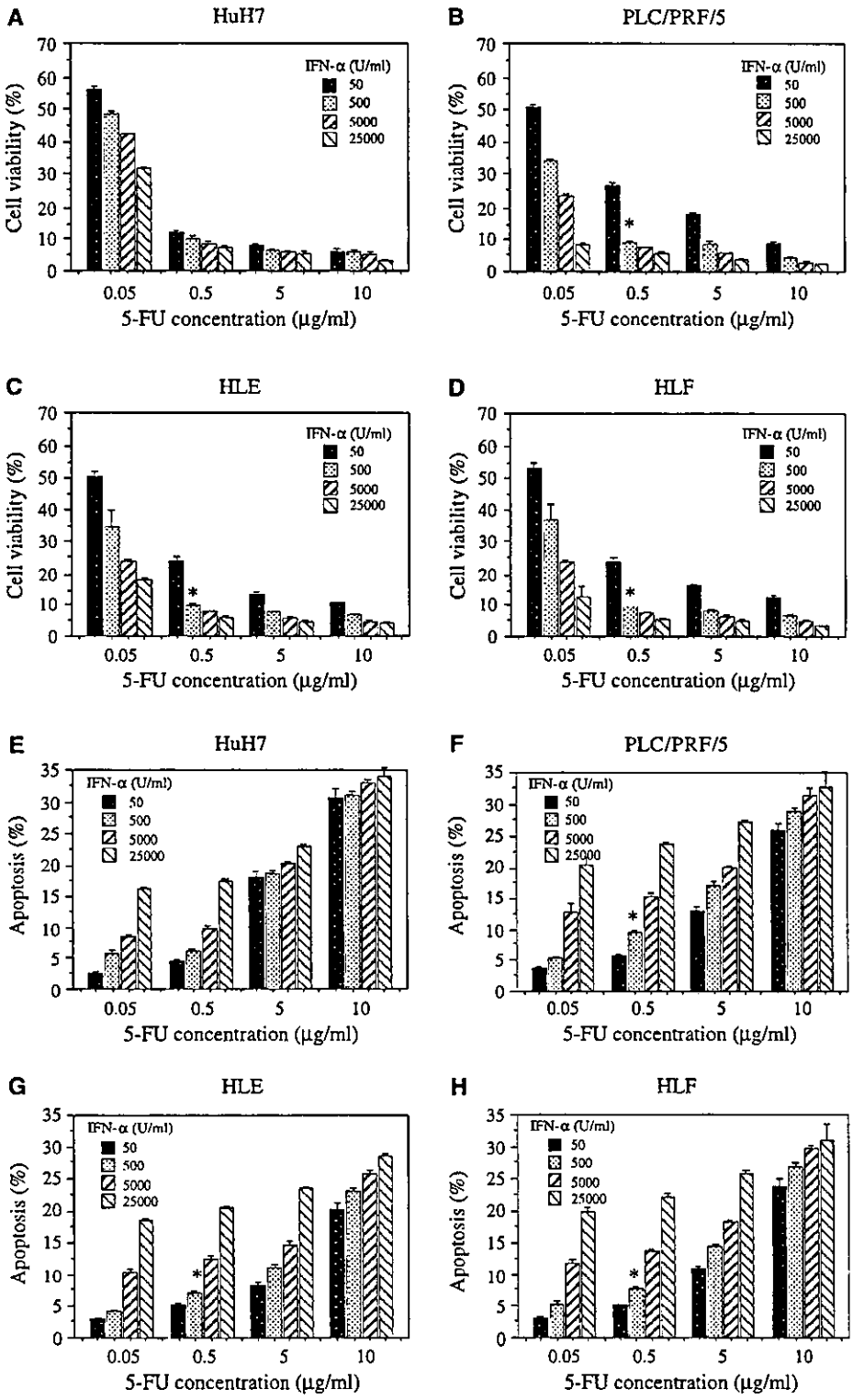

Fig. 2 Growth inhibitory effects (*A-D*) and incidence of apoptosis (*E-H*) of IFN-α in combination of various doses of 5-FU. Cells were incubated with IFN-α in the presence of various concentrations of 5-FU, and cell growth and apoptosis were determined on day 10 as described in Materials and Methods. When IFN-α and 5-FU were administered simultaneously, the antiproliferative effects and induction of apoptosis were higher than those of each drug alone in all cell lines (compared with Fig. 1). Mean (*columns*) ± SE (*bars*). *, $P < 0.05$, significant synergistic effect as examined by isobologram analysis.

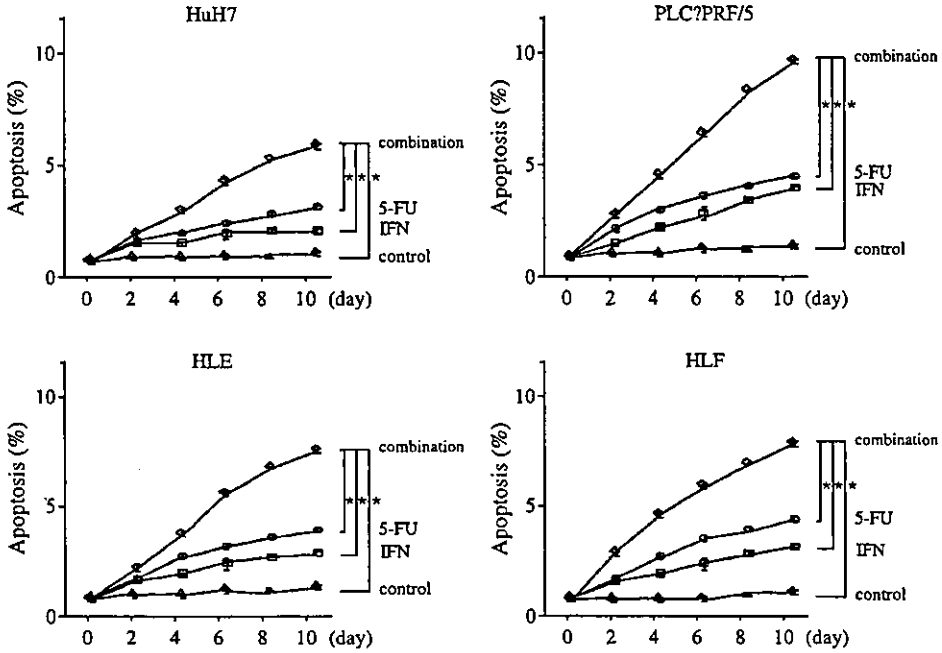

Fig. 3 Growth curves were drawn up to day 10 for the four HCC cell lines untreated or treated with 500 units/mL IFN-α and/or 0.5 μg/mL 5-FU. There was a significant difference in the number of PLC/PRF/5, HuH7, HLE, and HLF at day 10 among control, IFN-α, 5-FU, and their combination groups. Mean (*points*) ± SE (*bars*). *, $P < 0.05$.

(0.5 μg/mL) alone showed significant DNA fragmentation on day 10 (Fig. 5), although this was relatively weak in HuH7 cells. In comparison, DNA fragmentation was strong in PLC/PRF/5 and moderate in HLE and HLF. The experiments were repeated five times for evaluation and the results were reproducible.

Combination Therapy Increases Cytochrome c Expression. Expression of cytochrome *c* was confirmed in all cell lines. Combination therapy enhanced the expression of cytochrome *c*. This was relatively strong in PLC/PRF/5 but weak in HuH7 and moderate in HLE and HLF (Fig. 6*A*). Expression of cytochrome *c* in HuH7, PLC/PRF/5, HLE, and HLF treated with combination therapy were higher than IFN-α- and 5-FU-treated cells and these changes were not statistically significant (Fig. 6*A*). Restimulation every 48 hours by combination therapy induced up-regulation of cytochrome *c* in HuH7 (Fig. 6*B*). Enhanced expression of cytochrome *c* was not statistically significant on each day. The experiments were repeated five times for analysis and the results were reproducible.

IFN-α, 5-Fluorouracil, and Combination Therapy Enhance Expression of Apoptosis-Related Proteins. Cells were stimulated for 10 days with 500 units/mL IFN-α and/or 0.5 μg/mL 5-FU. Free cells in the medium were harvested every 48 hours and those attached to the dish were harvested 10 days later. The experiments were repeated five times for analysis. The results were summarized in Table 1.

Expression of Bax was confirmed in all cell lines. Combination therapy enhanced the expression by 3.47 times in HuH7, 3.72 times in PLC/PRF/5, 2.09 times in HLE, and 1.38 times in HLF. Expression levels of Bax in IFN-α plus 5-FU–treated HuH7, PLC/PRF/5, and HLE, but not HLF, cells on day 10 were significantly higher than those of IFN-α and 5-FU groups ($P < 0.05$).

In similar studies, the cells were stimulated and the value of Bcl-2 band relative to actin band was calculated. The intensities of the bands were analyzed densitometrically. Expression of Bcl-2 was confirmed in all cell lines. Combination of IFN-α and 5-FU enhanced the expression by 1.01 times in HuH7, decreased by 5.21 times in PLC/PRF/5, decreased by 7.64 times in HLE, and decreased by 1.60 times in HLF. Expression levels of Bcl-2 on PLC/PRF/5, HLE, and HLF treated with combination therapy on day 10 were lower than IFN-α- and 5-FU-treated cells, although these changes were not statistically significant.

In another analysis, expression of Bcl-x_L was confirmed in all cell lines. Combination therapy decreased the expression by 1.39 times in HuH7, 5.77 times in PLC/PRF/5, 3.13 times in HLE, and 4.86 times in HLF. The effects of IFN-α, 5-FU, and combination therapy on day 10 on the expression of Bcl-x_L on PLC/PRF/5, HLE, and HLF varied significantly ($P < 0.05$), but the effect of such treatments on Bcl-x_L expression in HuH7 was not different.

Expression of IFN-α/βR on Hepatocellular Carcinoma Cell Lines. The IFN-α/βR (long form plus short form) band relative to actin band was calculated. The relative ratio of IFN-α/βR in HuH7, PLC/PRF/5, HLE, and HLF were 0.34, 0.61, 0.49, and 0.54, respectively (Table 1). Expression of IFN-α/βR protein on the cell surface was observed in all cell lines, although it was relatively weak in HuH7 cells. The IFN-α/βR level was strong in PLC/PRF/5 and moderate in HLE and HLF. The expression level of IFN-α/βR protein on the cell surface in PLC/PRF/5 was statistically higher than that of HuH7 but not HLE and HLF. The experiments were repeated five times for analysis and the results were reproducible.

Combination Therapy Increases IFN-α/βR Signaling Protein Expression. Cells were stimulated for 30 minutes with 500 units/mL IFN-α or 0.5 μg/mL 5-FU or their combination and the relative value of α-phospho-STAT1 or IRF-1 band to actin band was calculated. The relative expression data for each treatment group are shown in Table 1. Combination therapy enhanced the expression of α-phospho-STAT1 by 1.04 times in HuH7, 2.82 times in PLC/PRF/5, 2.00 times in HLE, and 1.79 times in HLF. In comparison, 500 units/mL IFN-α enhanced the expression by 1.03 times in HuH7, 2.79 times in PLC/PRF/5,

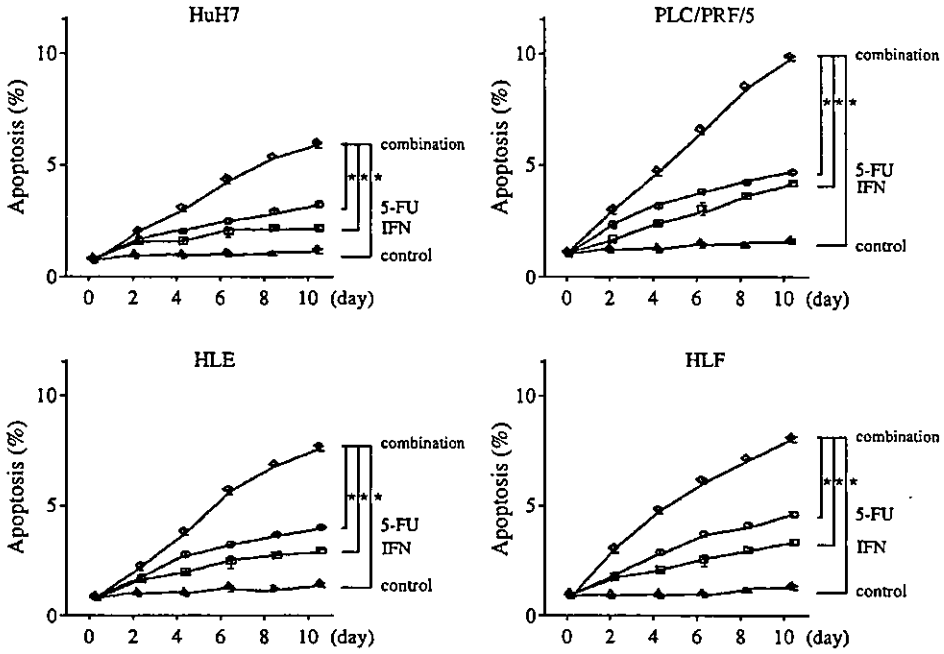

Fig. 4 TUNEL assays were done 10 days after the addition of IFN-α (500 units/mL), 5-FU (0.5 μg/mL), or their combination to detect apoptotic cells. TUNEL analysis showed a significant difference in cell numbers at day 10 between the combination therapy group and other treatment groups. Mean (*points*) ± SE (*bars*). *, $P < 0.05$.

1.98 times in HLE, and 1.77 times in HLF. However, 0.5 μg/mL 5-FU did not enhance the expression.

Combination therapy enhanced the expression of IRF-1 by 2.01 times in HuH7, 3.52 times in PLC/PRF/5, 2.81 times in HLE, and 3.01 times in HLF. In comparison, 500 units/mL IFN-α enhanced the expression by 1.51 times in HuH7, 3.12 times in PLC/PRF/5, 2.32 times in HLE, and 2.69 times in HLF. However, 0.5 μg/mL 5-FU did not enhance the expression.

Expression of α-phospho-STAT1 and IRF-1 in HuH7, PLC/PRF/5, HLE, and HLF treated with combination therapy were higher than IFN-α-treated cells and these changes were not statistically significant. Expression of α-phospho-STAT1 and IRF-1 by combination therapy in PLC/PRF/5 was statistically higher than that of HuH7 but not HLE and HLF.

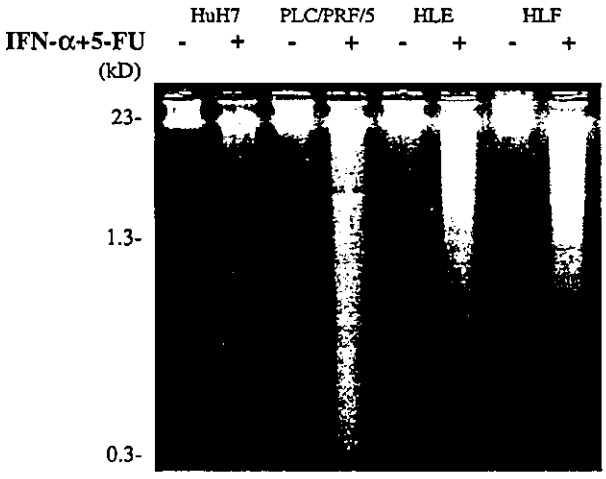

Fig. 5 DNA fragmentation. Cells were treated with or without the combination of 500 units/mL IFN-α and 0.5 μg/mL 5-FU for 10 days. DNA was isolated and analyzed as described in Materials and Methods.

Increased Apoptosis of IFNAR2c-Transfected HuH7 Cells. The expression of IFNAR2c protein was weak on HuH7 cells but strong on IFNAR2c transfected HuH7 (Fig. 7*A*). Nontransfected HuH7 treated with IFN-α (500 units/mL) and 5-FU (0.5 μg/mL) showed weak DNA fragmentation, whereas transfected HuH7 showed strong DNA fragmentation (Fig. 7*B*). Furthermore, DNA fragmentation of transfected HuH7 treated with combination therapy was stronger than IFN-α- and 5-FU-treated cells (Fig. 7*B*). Control experiments indicated that transfection reagents did not induce apoptosis (data not shown). The experiments were repeated thrice for evaluation and the results were reproducible.

Correlation of Several Factors. Relatively strong expression of IFN-α/βR, strong up-regulation of α-phospho-STAT1 and IRF-1, strong induction of apoptosis, and strong cell growth inhibition were observed in PLC/PRF/5 treated with combination therapy. On the other hand, the same treatment produced relatively weak or moderate changes in HuH7, HLE, and HLF cells. Moreover, almost all Bcl-2 protein family in all cell lines changed to induce apoptosis. Down-regulation of Bcl-x_L by combination therapy was correlated with the extent of apoptosis in all cell lines.

DISCUSSION

Previous studies suggested that combination chemotherapy of IFN-α, 5-FU, and other agents was to some extent useful to suppress advanced HCC (14, 20, 31–36). Based on these results, the present *in vitro* study was done in an effort to explore the underlying mechanisms of combination therapy. The major findings of the present study were as follows: (*a*) combination therapy inhibited cell growth and induced apoptosis of HCC cells in a dose- and time-dependent manner; (*b*) Bcl-2 family plays a key role in combination therapy–related apoptosis; (*c*) inhibition of cell growth and induction of apoptosis were

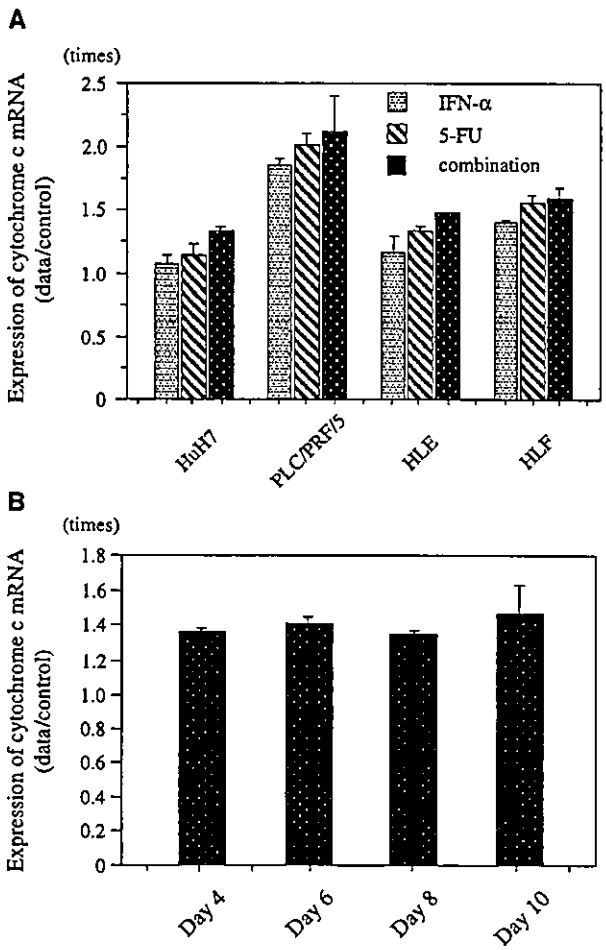

Fig. 6 Detection of cytochrome *c* by LightCycler. *A*, cells were treated with 500 units/mL IFN-α or 0.5 μg/mL 5-FU or their combination for 48 hours. Cytochrome *c* was up-regulated by combination therapy in all cell lines. *B*, time course results of restimulation by combination therapy in HuH7 cells. Cytochrome *c* was up-regulated after each restimulation. Mean (*columns*) ± SE (*bars*).

synergistic or additive but not antagonistic; (*d*) IFN-α/βR expression was frequently observed on HCC cells, although its signaling protein, α-phospho-STAT1 and IRF-1, were up-regulated by combination therapy; and (*e*) *IFNAR2c* gene transfer with combination therapy induced strong DNA fragmentation.

In the present study, the cell growth of HuH7, PLC/PRF/5, HLE, and HLF treated with 500 units/mL IFN-α and 0.5 μg/mL 5-FU for 10 days was significantly suppressed compared with cells treated with IFN-α alone or 5-FU alone (Fig. 3). Furthermore, the reduction rate of cell growth in each cell line was >80%. In our department, prospective clinical trials using IFN-α and 5-FU have been in progress since 1997 for patients with inoperable and extremely advanced HCC who were predicted to die within 3 to 6 months. Although these studies should continue for several more years, we have thus far obtained satisfactory results with this protocol (data not shown). Preliminary data indicated that >70% of patients who received the combination therapy developed a partial or complete

Table 1 Relative expression data of the each proteins

	HuH7	PLC/PRF/5	HLE	HLF
IFN				
IRN-R	0.34	0.61	0.49	0.54
p-STAT1	1.03	2.79	1.98	1.77
IRF-1	1.51	3.12	2.32	2.69
Bax	1.03	1.25	1.13	1.20
Bcl-2	0.96	0.28	0.27	0.78
Bcl-x_L	0.81	0.54	0.84	0.56
5-FU				
p-STAT1	1.00	1.01	1.00	1.01
IRF-1	1.01	1.00	1.01	1.00
Bax	2.21	2.24	1.23	1.24
Bcl-2	1.05	0.26	0.25	0.68
Bcl-x_L	0.76	0.38	0.56	0.41
p-STAT1	1.04	2.82	2.00	1.79
IFN + 5-FU				
IRF-1	2.01	3.52	2.81	3.01
Bax	3.47	3.72	2.09	1.38
Bcl-2	1.01	0.19	0.13	0.62
Bcl-x_L	0.72	0.17	0.32	0.21

response and that responders survived longer than we had expected (14). These effects are similar to the present *in vitro* results. Recently, we reported that up-regulation of $p27^{Kip1}$ was one of the direct mechanisms of combination therapy–mediated antitumor effects (19). In this regard, previous studies showed that IFN-α reduced 5-FU clearance and altered 5-FU metabolism (i.e., increased the amount of 5-fluoro-dUMP that can bind to thymidylate synthetase), resulting in inhibition of conversion of dUMP to dTMP during normal DNA synthesis (15, 16). It seems that IFN-α reduces the uptake of thymidine and the activity of thymidine kinase in conjunction with the action of 5-FU. Changes in the 5-FU metabolic pathway could be one of the underlying mechanism of IFN-α synergism. In this context, Kaneko et al. (20) recently reported that the thymidylate

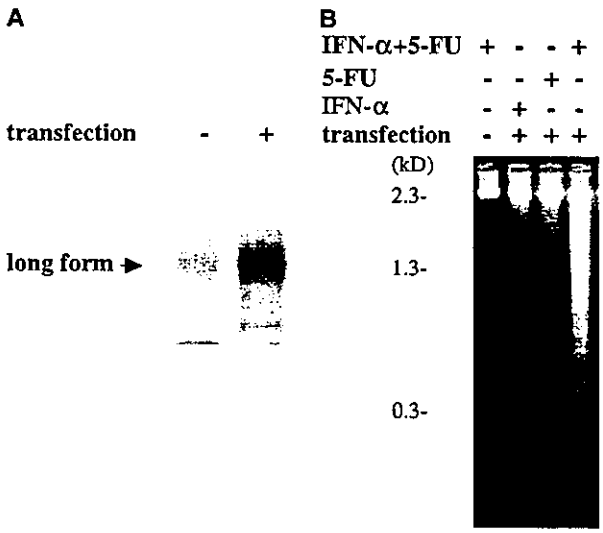

Fig. 7 *A*, transfection of IFNAR2c in HuH7 increased expression of IFNAR2c on the cell surface. In comparison, a weak IFNAR2c was noted in nontransfected HuH7 cells. *B*, strong DNA fragmentation was observed by combination therapy in IFNAR2c-transfected but not in nontransfected HuH7 cells.

synthetase inhibition rate was increased and the amount of 5-fluoro-dUMP was decreased following treatment with IFN-α and 5-FU in HuH7 cells.

To determine the effect of combination therapy on apoptosis in mechanistic study, TUNEL assay was done 10 days after treatment of 500 units/mL IFN-α and 0.5 μg/mL 5-FU. Importantly, the concentration of 5-FU used in our study was almost the same as that in plasma of patients treated by continuous infusion (23). As shown in this study, the proportions of apoptotic cells in each cell lines treated with IFN-α and 5-FU for 10 days were <10%. However, the proportions of apoptotic cells accumulated in a time-dependent manner, indicating that induction of apoptosis is one of the direct underlying mechanisms of this therapy. Our earlier studies indicated that apoptosis assay did not explain the synergistic effects of IFN-α and 5-FU in PLC/PRF/5 (19). This apparent discrepancy is a reflection of the length of exposure of the cells to the drugs. The cells were incubated with the drugs for 10 days in the present study, whereas the cells were incubated for only 3 days in our previous study (19).

To examine the mechanism of apoptosis, we examined the expression of Bcl-2 protein family, which is an important regulator of apoptosis (37). Recent studies suggested that regulation of apoptotic pathways by STATs is largely mediated by transcriptional activation of genes that encode proteins that mediate or trigger the cell death process, such as Bcl-2 protein family (38, 39). In the present study, Bcl-2 protein family induced apoptosis (i.e., combination therapy increased the expression of Bax and reduced the expression of Bcl-2 and Bcl-x_L; Table 1). Moreover, combination therapy also up-regulated α-phospho-STAT1 expression. These results suggest that combination therapy induces Bcl-2 family-related apoptosis. In this regard, it is considered that α-phospho-STAT1 might bind to the direct-responsive element of Bcl-2 family on HCC cells to induce apoptosis (39). Many cancer cells express either Bcl-2 or Bcl-x_L and these apoptosis-suppressing proteins as well as other Bcl-2 protein family have been implicated in resistance and susceptibility to anticancer therapy (40–42). For example, overexpression of Bcl-x_L is an important factor in 5-FU resistance in human colon and breast cancer cell lines (42, 43). In our study, down-regulation of Bcl-x_L was correlated with the incidence of apoptosis. One possible explanation for the synergistic or additive effects could be suggested. Up- or down-regulation of Bcl-2 protein family, especially Bcl-x_L, by IFN-α might relate with up-regulation of 5-FU sensitivity.

Cytochrome *c* levels are regulated by balanced expression of Bcl-2 family of proteins. Released cytochrome *c* binds Apaf-1 and caspase-9 and induces apoptosis (44). As shown in this study, cytochrome *c* mRNA was up-regulated by combination therapy. Our data indicate that changes in expression levels of Bcl-2 family result in activation of cytochrome *c* and consequently lead to apoptosis. This conclusion is based on the similar pattern of apoptosis and up-regulation of cytochrome *c* levels. Furthermore, our data showed that restimulation by combination therapy increased the expression of cytochrome *c*, indicating that the cooperative effects of combination therapy might be observed clinically on re-medication.

On the other hand, it is well known that IFN-α exerts its effect through the specific cell surface receptor, IFN-α/βR, which subsequently activates Janus-activated kinase/STAT pathway. In fact, the expression levels of IFN-α/βR mRNA and protein have been studied in liver tissues of viral hepatitis and their expression can predict the efficacy of IFN therapy in chronic hepatitis (45–47). Furthermore, we reported that IFN-α/βR is expressed not only in chronic hepatitis and liver cirrhosis but also in HCC (48). IFN-α has a variety of antitumor effects, including immunomodulation, inhibition of angiogenesis, and antiproliferative activity through the binding to its high-affinity membrane receptor, IFN-α/βR, which results in activation of STATs, leading to antiproliferative or apoptotic effects in concert with IRFs (49). Our results showed that IFN-α/βR is expressed in HCC cells and that combination therapy up-regulated IFN-α/βR signaling protein, α-phospho-STAT1, and IRF-1. These results suggest that up-regulation of α-phospho-STAT1 and IRF-1 are directly related to the inhibition of HCC cell growth. Interestingly, our preliminary study indicated that the effects of combination therapy correlated with the level of expression of IFN-α/βR (data not shown).

To address whether increased expression of IFN-α/βR *in vitro* is associated with a higher biological response to combination therapy, we conducted the IFNAR2c-transfected study. In this study, we used HuH7 cells, which have low expression level of IFNAR2c. Our results showed that after temporary transfection of IFNAR2c, combination therapy induced strong DNA fragmentation compared with non-transfected HuH7 (Fig. 7*B*). Moreover, increased expression of α-phospho-STAT1 was observed (data not shown). To our knowledge, this is the first report of *IFNAR2c* gene transfer being effective in augmenting the biological activity of combination therapy in human HCC. Our results strongly suggest that *IFN-α/βR* gene transfer with combination therapy could be potentially useful clinically in patients with HCC.

In conclusion, we have shown in the present study that combination of IFN-α plus 5-FU induced strong inhibition of cell growth with Bcl-2 family-associated apoptosis. The results suggested that expression of IFN-α/βR and signal transduction might be important mechanisms of action of this therapy.

REFERENCES

1. Grazi GL, Ercolani G, Pierangeli F, et al. Improved results of liver resection for hepatocellular carcinoma on cirrhosis give the procedure added value. Ann Surg 2001;234:71–8.

2. Nagasue N, Ono T, Yamanoi A, et al. Prognostic factors and survival after hepatic resection for hepatocellular carcinoma without cirrhosis. Br J Surg 2001;88:515–22.

3. Landis SH, Murray T, Bolden S, Wingo PA. Cancer statistics, 1999. CA Cancer J Clin 1999;49:8–31.

4. Furuse J, Iwasaki M, Yoshino M, et al. Hepatocellular carcinoma with portal vein tumor thrombus: embolization of arterioportal shunts. Radiology 1997;204:787–90.

5. Lin DY, Lin SM, Liaw YF. Non-surgical treatment of hepatocellular carcinoma. J Gastroenterol Hepatol 1997;12:S319–28.

6. Ikai I, Yamaoka Y, Yamamoto Y, et al. Surgical intervention for patients with stage IV-A hepatocellular carcinoma without lymph node metastasis: proposal as a standard therapy. Ann Surg 1998;227:433–9.

7. Miyamoto A, Umeshita K, Sakon M, et al. A case of advanced hepatocellular carcinoma with lung metastasis, successfully treated by a combination therapy with interferon and UFT, an oral antineoplastic agent combining tegafur and uracil. J Gastroenterol Hepatol 2000;15:1447–51.

8. Wadler S, Schwartz EL, Goldman M, Lyver A, Itri L, Wiernik PH. Preclinical and clinical studies of 5-fluorouracil (FURA) and recombinant α-2a-interferon (IFN) against gastrointestinal (GI) malignancies. Clin Res 1988;36:803A.

9. Wadler S, Schwartz EL, Goldman M, et al. Fluorouracil and recombinant α-2a-interferon: an active regimen against advanced colorectal carcinoma. J Clin Oncol 1989;7:1769–75.

10. Wadler S, Schwartz EL. Antineoplastic activity of the combination of interferon and cytotoxic agents against experimental and human malignancies: a review. Cancer Res 1990;50:3473–86.

11. Greenblatt MS, Mangalik A, Ferguson J, Elias L. Phase I evaluation of therapy with four schedules of 5-fluorouracil by continuous infusion combined with recombinant interferon α. Clin Cancer Res 1995;1:615–20.

12. Kelsen D, Lovett D, Wong J, et al. Interferon α-2a and fluorouracil in the treatment of patients with advanced esophageal cancer. J Clin Oncol 1992;10:269–74.

13. Lee KH, Lee JS, Suh C, et al. Combination of 5-fluorouracil and recombinant interferon α-2B in advanced gastric cancer. A phase I study. Am J Clin Oncol 1992;15:141–5.

14. Sakon M, Nagano H, Dono K, et al. Combined intraarterial 5-fluorouracil and subcutaneous interferon-α therapy for advanced hepatocellular carcinoma with tumor thrombi in the major portal branches. Cancer 2002;94:435–42.

15. Schwartz EL, Hoffman M, O'Connor CJ, Wadler S. Stimulation of 5-fluorouracil metabolic activation by interferon-α in human colon carcinoma cells. Biochem Biophys Res Commun 1992;182:1232–9.

16. Elias L, Sandoval JM. Interferon effects upon fluorouracil metabolism by HL-60 cells. Biochem Biophys Res Commun 1989;163:867–74.

17. Matheson DS, Green BJ, Friedman SJ, Hoar DI. Studies on the mechanism of activation of human natural killer function by interferon and inhibitors of thymidylate synthesis. Cell Immunol 1988;111: 118–25.

18. Sabaawy HE, Farley T, Ahmed T, Feldman E, Abraham NG. Synergetic effects of retrovirus IFN-α gene transfer and 5-FU on apoptosis of colon cancer cells. Acta Haematol 1999;101:82–8.

19. Eguchi H, Nagano H, Yamamoto H, et al. Augmentation of antitumor activity of 5-fluorouracil by interferon α is associated with up-regulation of $p27^{Kip1}$ in human hepatocellular carcinoma cells. Clin Cancer Res 2000;6:2881–90.

20. Kaneko S, Urabe T, Kobayashi K. Combination chemotherapy for advanced hepatocellular carcinoma complicated by major portal vein thrombosis. Oncology 2002;62:69–73.

21. Damdinsuren B, Nagano H, Sakon M, et al. Interferon-β is more potent than interferon-α in inhibition of human hepatocellular carcinoma cell growth when used alone and in combination with anticancer drugs. Ann Surg Oncol 2003;10:1184–90.

22. Yamamoto H, Soh JW, Monden T, et al. Paradoxical increase in retinoblastoma protein in colorectal carcinomas may protect cells from apoptosis. Clin Cancer Res 1999;5:1805–15.

23. Fraile RJ, Baker LH, Buroker TR, Horwitz J, Vaitkevicius VK. Pharmacokinetics of 5-fluorouracil administered orally, by rapid intravenous and by slow infusion. Cancer Res 1980;40:2223–8.

24. Wittwer CT, Ririe KM, Andrew RV, David DA, Gundry RA, Balis UJ. The LightCycler: a microvolume multisample fluorimeter with rapid temperature control. Biotechniques 1997;22:176–81.

25. Miyake Y, Fujiwara Y, Ohue M, et al. Quantification of micrometastases in lymph nodes of colorectal cancer using real-time fluorescence polymerase chain reaction. Int J Oncol 2000;16:289–93.

26. Miyamoto A, Nagano H, Sakon M, et al. Clinical application of quantitative analysis for detection of hematogenous spread of hepatocellular carcinoma by real-time PCR. Int J Oncol 2000;18: 527–32.

27. Chandra D, Liu JW, Tang DG. Early mitochondrial activation and cytochrome *c* up-regulation during apoptosis. J Biol Chem 2002;277: 50842–54.

28. Pals G, Pindolia K, Worsham MJ. A rapid and sensitive approach to mutation detection using real-time polymerase chain reaction and melting curve analyses, using BRCA1 as an example. Mol Diagn 1999; 4:241–6.

29. Miyata H, Doki Y, Yamamoto Y, et al. Overexpression of CDC25B overrides radiation-induced G_2-M arrest and results in increased apoptosis in esophageal cancer cells. Cancer Res 2001;61:3188–93.

30. Kimura Y, Shiozaki H, Doki Y, et al. Cytoplasmic β-catenin in esophageal cancers. Int J Cancer 1999;84:174–8.

31. Patt YZ, Yoffe B, Charnsangavej C, et al. Low serum α-fetoprotein level in patients with hepatocellular carcinoma as a predictor of response to 5-FU and interferon-α-2b. Cancer 1993;72:2574–82.

32. Urabe T, Kaneko S, Matsushita E, Unoura M, Kobayashi K. Clinical pilot study of intrahepatic arterial chemotherapy with methotrexate, 5-fluorouracil, cisplatin and subcutaneous interferon-α-2b for patients with locally advanced hepatocellular carcinoma. Oncology 1998;55:39–47.

33. Leung TW, Patt YZ, Lau WY, et al. Complete pathological remission is possible with systemic combination chemotherapy for inoperable hepatocellular carcinoma. Clin Cancer Res 1999;5:1676–81.

34. Komorizono Y, Kohara K, Oketani M, et al. Systemic combined chemotherapy with low dose of 5-fluorouracil, cisplatin, and interferon-α for advanced hepatocellular carcinoma: a pilot study. Dig Dis Sci 2003; 48:877–81.

35. Yuen MF, Ooi CG, Hui CK, et al. A pilot study of transcatheter arterial interferon embolization for patients with hepatocellular carcinoma. Cancer 2003;97:2776–82.

36. Ohmoto K, Iguchi Y, Mimura N, et al. Combined intraarterial 5-fluorouracil and intramuscular interferon-α therapy for advanced hepatocellular carcinoma. Hepatogastroenterology 2003;50:1780–82.

37. Adams JM, Cory S. The Bcl-2 protein family: arbiters of cell survival. Science 1998;281:1322–6.

38. Battle TE, Frank DA. The role of STATs in apoptosis. Curr Mol Med 2002;2:381–92.

39. Stephanou A, Brar BK, Knight RA, Latchman DS. Opposing actions of STAT-1 and STAT-3 on the Bcl-2 and Bcl-x promoters. Cell Death Differ 2000;7:329–30.

40. Zhang L, Yu J, Park BH, Kinzler KW, Vogelstein B. Role of BAX in the apoptotic response to anticancer agents. Science 2000; 290:989–92.

41. Sjostrom J, Blomqvist C, von Boguslawski K, et al. The predictive value of bcl-2, bax, bcl-x_L, bag-1, fas, and fasL for chemotherapy response in advanced breast cancer. Clin Cancer Res 2002;8:811–6.

42. Nita ME, Nagawa H, Tominaga O, et al. 5-Fluorouracil induces apoptosis in human colon cancer cell lines with modulation of Bcl-2 family proteins. Br J Cancer 1998;78:986–92.

43. Liu R, Page C, Beidler DR, Wicha MS, Nunez G. Overexpression of Bcl-x(L) promotes chemotherapy resistance of mammary tumors in a syngeneic mouse model. Am J Pathol 1999;155:1861–7.

44. Li P, Nijhawan D, Budihardjo I, et al. Cytochrome *c* and dATP-dependent formation of Apaf-1/caspase-9 complex initiates an apoptotic protease cascade. Cell 1997;91:479–89.

45. Fukuda R, Ishimura N, Kushiyama Y, et al. Effectiveness of interferon-α therapy in chronic hepatitis C is associated with the amount of interferon-α receptor mRNA in the liver. J Hepatol 1997;26:455–61.

46. Mizukoshi E, Kaneko S, Yanagi M, et al. Expression of interferon α/β receptor in the liver of chronic hepatitis C patients. J Med Virol 1998;56:217–23.

47. Yatsuhashi H, Fujino T, Matsumoto T, Inoue O, Koga M, Yano M. Immunohistochemical analysis of hepatic interferon α-β receptor level: relationship between receptor expression and response to interferon therapy in patients with chronic hepatitis C. J Hepatol 1999;30:995–1003.

48. Kondo M, Nagano H, Sakon M, et al. Expression of interferon α/β receptor in human hepatocellular carcinoma. Int J Oncol 2000;17:83–8.

49. Harada H, Kitagawa M, Tanaka N, et al. Anti-oncogenic and oncogenic potentials of interferon regulatory factors-1 and -2. Science 1993;259:971–4.

Akt2 expression correlates with prognosis of human hepatocellular carcinoma

XUNDI XU[1], MASATO SAKON[1], HIROAKI NAGANO[1], NOBUAKI HIRAOKA[1], HIROFUMI YAMAMOTO[1], NOBUYASU HAYASHI[1], KEIZO DONO[1], SHOJI NAKAMORI[1], KOJI UMESHITA[1], YASUHIRO ITO[1], NARIAKI MATSUURA[2] and MORITO MONDEN[1]

[1]Department of Surgery and Clinical Oncology, Graduate School of Medicine; [2]Department of Pathology, School of Allied Health Science, Faculty of Medicine, Osaka University, Osaka 565-0871, Japan

Received July 29, 2003; Accepted September 3, 2003

Abstract. Akt, a down-stream target of phosphatidylinositol-3 kinase, plays multiple roles in carcinogenesis. To elucidate its role in hepatocarcinogenesis, we immunohistochemically investigated the expression of Akt protein (Akt1 and Akt2) in tumor and non-tumor tissues from 56 patients with hepatocellular carcinoma (HCC). High expression of Akt2 in HCC tissues was detected in 21 cases (38%) while Akt1 expression was moderate or less in all cases. Low expression of Akt2 was associated with histopathological differentiation, portal invasion and number of tumor nodules (p=0.026, 0.023, and 0.001, respectively). Univariate analysis showed that Akt2, histopathological differentiation, and portal vein invasion were significant prognostic factors (p=0.001, 0.028, and 0.006, respectively). Multivariate analysis revealed that in addition to histopathological differentiation, Akt2 was an independent prognostic marker (risk ratio for cancer relapse, 6.35, p=0.012). In contrast, Akt1 expression did not correlate with any clinicopathological features. Our findings suggest that Akt2, but not Akt1, is a novel independent predictor for the development and progression of HCC.

Introduction

Primary hepatocellular carcinoma (HCC) is currently the 5th most common cancer worldwide and its incidence is rising due to infection with hepatitis B and C viruses. In the USA, the incidence of histologically proven HCC has risen from 1.4/100,000/year population in 1975 to 2.4/100,000/year population between the years 1991-1995, together with a decrease in the median age of onset (1,2). Despite the development of various therapeutic modalities, the prognosis of HCC is still unsatisfactory (3). Therefore, it is essential to elucidate the prognostic factors for this disease, particularly in resectable cases where surgical stress and reduced liver function due to hepatectomy cannot be ignored.

Recent molecular approaches have revealed the involvement of alteration of various genes, such as *β-catenin, cyclin D1, $p27^{KIP1}$, Rb* and *p53*, in hepatocarcinogenesis (4-7), however details of the intracellular signaling mechanisms are not available at present. The serine/threonine kinase Akt (or Akt/PKB) is a direct down-stream target of phosphatidylinositol-3 kinase (PI-3 kinase), which is activated by various growth factors (8,9). To date, 3 major isoforms of Akt/PKB; Akt1/PKB, Akt2/PKB and Akt3/PKB, have been identified, but Akt1 and Akt2 have been implicated in the development and progression of human cancers (10-12). Akt1 is located at chromosome band 14q32 proximal to the IGH locus, while human Akt2 maps to 19q13.1-q13.2 (13,14). The 2 genes have >85% sequence homology and share a common structure of their protein products (10-12). Since the pleckstrin homology domain of Akt has an affinity for PtdIns-3, 4-P2 and PtdIns-3,4,5-P3 (15,16), phosphorylation of PtdIns by PI-3 kinase triggers the translocation of Akt to the plasma membrane, leading to Akt/PKB kinase activation by autophosphorylation of Thr-308/309 and Ser-473/474 (17). Thus, Akt is considered to be involved in the regulation of various cellular processes, such as gene transcription, protein synthesis, glucose metabolism, and the cell cycle (18-20). In addition, Akt has been demonstrated to play an important role in various aspects of cancer development and progression such as anti-apoptosis, angiogenesis, unlimited replicative potential, tissue invasion and metastasis (21-26). Indeed, Akt is overexpressed in certain tumors, such as thyroid (27), ovarian (11,28), pancreatic (29) and gastric cancer (10). Akt1 kinase activity is increased in prostate and breast cancers and is associated with poor prognosis (30). However, the clinical significance of Akt in HCC has not been elucidated.

The present study was designed to determine the expression of Akt1 and Akt2 proteins in cancer and non-cancer tissues in patients with resectable HCC by immunohistochemistry.

Correspondence to: Dr Masato Sakon, Department of Surgery and Clinical Oncology, Graduate School of Medicine, Osaka University, 2-2 Yamada-oka, Suita City, Osaka 565-0871, Japan
E-mail: msakon@surg2.med.osaka-u.ac.jp

Abbreviations: HCC, hepatocellular carcinoma

Key words: hepatocellular carcinoma, Akt2, immunohistochemistry, Western blotting, prognosis

We also investigated the correlation between such expression and clinicopathologic features.

Materials and methods

Patients. Tissue samples and clinical data were obtained from 56 patients with HCC (43 males and 13 females; aged 31-76 years; mean 60±11.1 years), who underwent hepatectomy between 1993-1999 at the Department of Surgery and Clinical Oncology, Osaka University. Prior to hepatectomy, 33 patients were treated with trans-arterial embolization (TAE). All patients, except 4, had hepatitis C virus infection but none had hepatitis B virus infection. Patients were followed at least every 3 months by tumor marker analysis (α-fetoprotein and des-γ-carboxy prothrombin, PIVKA-II) and imaging studies such as abdominal ultrasonography or CT scan. The mean follow-up period was 3.6±1.5 years.

Histopathological examination. The resected surgical specimens were fixed in 10% neutral buffered formalin, processed through graded ethanol and embedded in paraffin. Tissue sections (4-μm thick) were deparaffinized in xylene, rehydrated with graded concentrations of ethanol and stained with hematoxylin and eosin (H&E) solution. The pathological diagnosis of non-tumor and tumor tissues was made by one of the authors (N.M.), who was blinded to the clinical background. For the 56 non-tumor tissues, the presence of active inflammation and cirrhotic nodules was assessed. We also examined 4 normal liver tissues, 23 chronic hepatitis (CH) and 29 liver cirrhosis (LC) tissues. Cancer tissues were microscopically examined for the following characteristics; cell differentiation (well-, moderately-, or poorly-differentiated), number of tumor nodules, capsular formation (fc), septal formation (sf), capsular invasion (fc inf), portal vein tumor thrombus formation (vp), and hepatic vein invasion (vv).

Antibodies. The goat polyclonal antibody for Akt1, mouse monoclonal antibody for Akt2 and their blocking peptides were obtained from Santa Cruz Biotechnology (Santa Cruz, CA) (29,31).

Immunohistochemistry. Immunostaining was performed with a standard avidin-biotin complex (ABC) method, using the Vectastain ABC-peroxidase kit (Vector Laboratories, Burlingame, CA), as described previously (32). The primary antibodies were applied to the sections at the following dilutions: anti-Akt1 antibody, 1:200 and anti-Akt2 antibody, 1:200. For the positive controls of Akt2, sections of ovarian cancer with strong expression of Akt protein (28) were included in each staining procedure (data not shown). For negative controls, phosphate-buffered saline (PBS) was used as a substitute for the primary antibody to verify the possibility of false positive responses. In addition, absorption tests with blocking peptides were performed to verify the specificity of the Akt1 and Akt2 antibodies.

All immunostained sections were evaluated in a coded manner by the principal author (X.X.) who was blinded to the clinical and pathological results of the patients. The expression of both Akt1 and Akt2 was predominantly found in the cytoplasm and the level of Akt protein expression was categorized semiquantitatively into 4 grades, 0 (none), 1 (faint), 2 (moderate), and 3 (intense). The staining level of Akt on epithelial cells of the bile ducts, which were devoid of significant inflammation and generally expressed Akt at a faint or moderate level, was used as an inner control within the sample. For statistical analysis, the intensity of Akt staining was scored using 2 scales. Akt1 staining was generally weak compared with that of Akt2, and therefore grade 1 or 2 was designated as 'high' expression while grade 0 was 'low'. For Akt2 protein expression, 'high expression' represented moderate (2) or intense (3) staining while 'low expression' indicated undetectable (0) or faint (1) staining.

In half of the samples, staining was repeated twice to avoid possible technical errors, and identical results were obtained in all cases. All slides were interpreted by 2 investigators (M.S. and N.M.) on different occasions. The results of interpretation were similar in over 90% of the samples. The final diagnosis of the remainder was made by these investigators using a multi-head microscope.

Western blot analysis. Cancer and non-cancer tissues were immediately frozen in liquid nitrogen and stored at -80°C for analysis by Western blotting. Approximately 100 mg of each sample was homogenized in 1 ml of lysis buffer [50 mM Tris (pH 8.0), 150 mM NaCl, and 0.5% NP40] with protease inhibitors (1 mM phenylmethylsulfonyl fluoride, 10 μg/ml aprotinin, and 10 μg/ml leupeptin). The homogenate was centrifuged at 13,000 rpm for 20 min at 4°C. The resulting supernatant was collected, and total protein concentration was determined using the Bradford protein assay (Bio-Rad, Hercules, CA). Western blotting was performed as described previously (32). Briefly, 50 μg of the total protein was subjected to 10% polyacrylamide gel electrophoresis (PAGE), followed by electroblotting onto a polyvinylidene difluoride membrane. After blocking in 5% skim milk, the membrane was incubated with 1 μg/ml Akt2 antibody, followed by incubation with the secondary antibody at a dilution of 1:2000. The enhanced chemiluminescence Western blot detection system (Amersham, Aylesbury, UK) was used to detect the immunocomplex.

Statistical analysis. Statistical analysis was performed using the Statview J-5.0 program (Abacus Concepts Inc., Berkeley, CA). The Kaplan-Meier method was used to estimate the survival rate. The log-rank test was used to examine the statistical difference in survival rates. The risk ratio under simultaneous contribution from several covariates was assessed by Cox's proportional hazards model. The associations between the discrete variables were assessed using the χ^2 test or Fisher's exact probability test. P-values <0.05 were accepted as statistically significant.

Results

Immunohistochemical analysis of Akt1 and Akt2. Staining for Akt1 protein was identified in the cytoplasm of both cancer and non-cancer cells (Fig. 1), but at a markedly lower level compared with Akt2 protein (Fig. 2). Sixteen of 56 non-cancer tissues (29%; 1 of 4 normal liver, 5 of 23 chronic hepatitis and 10 of 29 cirrhosis) exhibited low Akt1 protein